SOME NEW OBSERVATIONS IN ELECTRO-CHEMICAL SPARK MACHINING (ECSM) OF QUARTZ

By

Sanjoy Adhikary

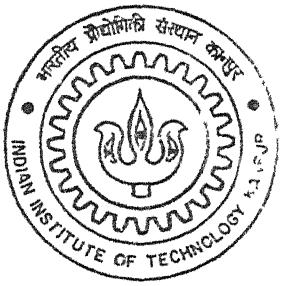

DEPARTMENT OF MECHANICAL ENGINEERING

Indian Institute of Technology Kanpur

MAY, 2003

SOME NEW OBSERVATIONS IN ELECTROCHEMICAL SPARK MACHINING (ECSM) OF QUARTZ

A thesis submitted in

Partial Fulfillment of the Requirements

For the Degree of

MASTER OF TECHNOLOGY

by

SANJOY ADHIKARY

to the

DEPARTMENT OF MECHANICAL ENGINEERING

INDIAN INSTITUTE OF TECHNOLOGY, KANPUR

MAY, 2003

CERTIFICATE

It is certified that work contained in the thesis entitled **SOME NEW OBSERVATIONS IN ELECTROCHEMICAL SPARK MACHINING (ECSM) OF QUARTZ,** by Mr Sanjoy Adhikary has been carried out under my supervision and this work has not been submitted elsewhere for a degree

May, 2003

Prof V K Jain
Department of Mechanical Engineering
I I T, Kanpur

DEDICATED TO

MY SISTERS

RUMI & SUMI

ABSTRACT

Machining of electrically non-conductive materials is still a major problem Electrochemical spark machining has potential for machining these materials compared with different existing traditional and also some non-traditional machining methods Despite the considerable amount of theoretical and experimental work that has been done related to this process, many fundamental aspects of the process are yet to understand and deficiencies of the process need to overcome Because of the complexity of the process, ECSM is still a process to be used on shop floor

In this present work, ECSM process has been applied successfully for cutting quartz plate Sharp edge tool and controlled feed of work-piece produces less overcut Reverse polarity cuts quartz plate at faster rate as compared to the direct polarity Surface finish along the cutting direction obtained is random in nature Minimum surface finish value obtained is quite good Tool wear in reverse polarity is much higher than direct polarity Electrochemical reactions responsible for material removal have been proposed Chemical analysis of reaction products also agrees with the feasibility of dissolution of quartz in solution Cutting also can be successfully done by using small auxiliary electrode Both the electrodes (cathode and anode) can also be simultaneously used as tool

ACKNOWLWDGEMENT

I express my unbound gratitude to Prof V K Jain for suggesting and deciding the problem I am deeply indebt to him for his meticulous guidance, devotion and inspiration throughout the tenure of this work

I am very thankful to Prof S Sarkar for his guidance and allowing me to do the chemical analysis in his lab

I am very grateful to the staff of manufacturing science laboratory, Mr R Thapliyal, Mr V Singh, Mr R Yadav, Mr A Gangwar, and Mr P C Gond for their consistent effort to make the set-up ready and their help during experiments

I am indebt to Mr sunil Jha for his help regarding instrumentation parts of the set-up I am very much thankful to Mr D K Singh, Mr D S Bilgi, Mr V K Gorana, Mr S C Jaiswal, Mr P M Pandey, Mr K Trimurthy, and Mr P V Kumar for their constant encouragement and for creating healthy academic environment in the lab

I am heartily thankful to Mr P dubey for helping me in chemical analysis

I am thankful to my batch mates specially, Mr Avisekh Banarjee, Mr Deepak Arzare, Mr Ravi Kumar and Ms Shaifali Mehrotra for making IIT kanpur memory full of fragrance

Last, but not least I am thankful to my childhood friends for their consistent encouragement at every difficult moment

CONTENTS

LIST OF FIGURES

LIST OF TABLES

Chapter 1

INTRODUCTION

Advanced ceramics and composites have tremendous potential for applications due to their superior properties such as high compressive strength, good thermal shock resistance, high wear resistance, high hardness, high strength to weight ratio, etc Such improved material properties, however, pose new challenges to manufacturing engineers to shape these materials economically and efficiently

Production of through and blind holes, grooves and slots, and complex shaped contours are difficult to obtain by traditional processes of compacting and sintering On the other hand, for the production of a small number of parts for devised applications of these materials is not economically viable to use mass production techniques such as casting and sintering It is, therefore believed that the field of utilization of these materials has remained comparatively narrow Electrical discharge machining (EDM) and Electro-Chemical machining (ECM) are the two electrically assisted advanced machining processes which are well established and are being successfully used in industries for machining electrically conductive materials

Diamond grinding, ultrasonic machining, abrasive jet machining, abrasive water jet machining, laser beam machining, and ion beam machining are those processes which can be used for machining of electrically non-conductive materials also But these processes have their own limitations Electrochemical Spark Machining (ECSM) is a hybrid process that combines both ECM and EDM It can be successfully used for machining electrically non-conductive advanced materials

1.1 Basic principle of ECSM process

In ECSM process, cathode (i e tool) of the desired size and shape is 2-3 mm dipped in electrolyte and anode is usually a flat plate Both are kept at a distance of about 30-50 mm (Fig 1 1) Application of external potential (50-80 V) between the electrodes causes the flow of electric current through the cell, resulting the generation of hydrogen bubbles at cathode by electrochemical reactions Surface area of the cathode dipped in the electrolyte is very less compared to anode High current density at cathode surface results in rapid generation of hydrogen bubbles and shielding of cathode surface Boiling of electrolyte near small electrode occurs because of the heating of electrolyte due to high resistance to current flow Therefore an electrically non-conductive layer of gas-vapour mixture is formed and it shields the cathode surface Sparking occurs between cathode and electrolyte because of the breakdown of the insulating layer due to high potential gradient If the work-piece is brought to the vicinity of the spark zone, material removal from the tool and work-piece both will take place Thus sparking between tool and electrolyte is used to machine the material Material removal may be because of melting and vaporization, random thermal stresses and micro cracking, chemical reactions at high temperature and mechanical shock due to expanding gases

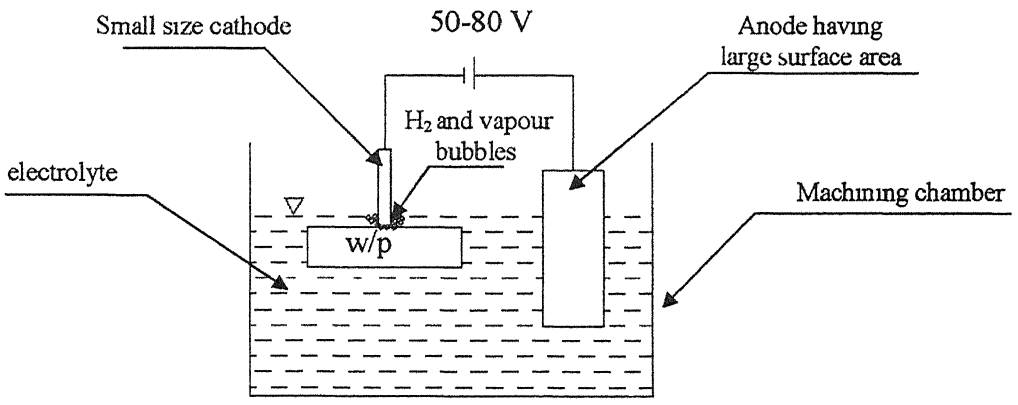

Fig 1 1 Schematic diagram of basic electrochemical cell in ECSM process

Reactions at Cathode and electrolyte interface:

The electrochemical reactions at cathode electrolyte interface cause evolution of hydrogen gas and deposition of copper

$Cu^{++} + 2e^- \rightarrow Cu$

$2H^+ + 2e^- \rightarrow H_2\uparrow$

$Na^+ + e^- \rightarrow Na$

$2Na + 2H_2O \rightarrow 2NaOH + H_2\uparrow$

$2H_2O + 2e^- \rightarrow H_2\uparrow + 2OH^-$

Here, hydrogen bubbles and vapor bubbles generated by boiling of electrolyte forms the insulating layer on anode surface

3.2 Dissolution of quartz

Schematic diagram of machining of quartz by ECSMWRP is shown in Fig 3 Reduction of silicon dioxide (SiO_2) occurs due to high electromotive force generated by high potential gradient A small gap between anode and work-piece also generates high resistance Sparking occurs due to high charge density and high resistance to current flow through anode-workpiece interface Heat generated by sparking accelerates the reduction process Freshly formed silicon is highly active and it is re-oxidized by fresh oxygen gas evolved at anode This newly precipitated SiO_2 is highly amorphous in nature and prone to chemical reactions [22] It reacts with sodium hydroxide to form sodium silicate and so dissolves into the NaOH solution and also forms copper silicate The reactions are as follows,

$SiO_2 + 4e^- + 4H^+ \rightarrow Si + 2H_2O$

$Si + O_2 \rightarrow SiO_2$

$SiO_2 + 2OH^- \rightarrow SiO_3^{--} + 2H_2O$

$Na^+ + SiO_3^{--} \rightarrow Na_2SiO_3 + Na_4SiO_4$

$Cu^{++} + SiO_3^{--} \rightarrow CuSiO_3$

1.2 Literature survey

In 1973, Cook et al [1] conducted experiments on various electrically non-conductive materials and observed that the process is highly sensitive to characteristics of the power supply and electrolyte They reported that machining rate increases with supply voltage, electrolyte concentration and electrolyte temperature But, for a given voltage, penetration rate decreases with time and hence leads to limited machined depth

In 1988, Allesu [2] carried out experiments on glass samples and proposed possible modes of material removal from workpiece viz, melting and vaporization, random thermal stress and microcracking, chemical reaction of silica at high temperature and mechanical shock wave generated by the cavitation effect He measured distribution of voltage drop between tool and electrode (Fig.1 2). He reported that discharge voltage increases in case of flowing

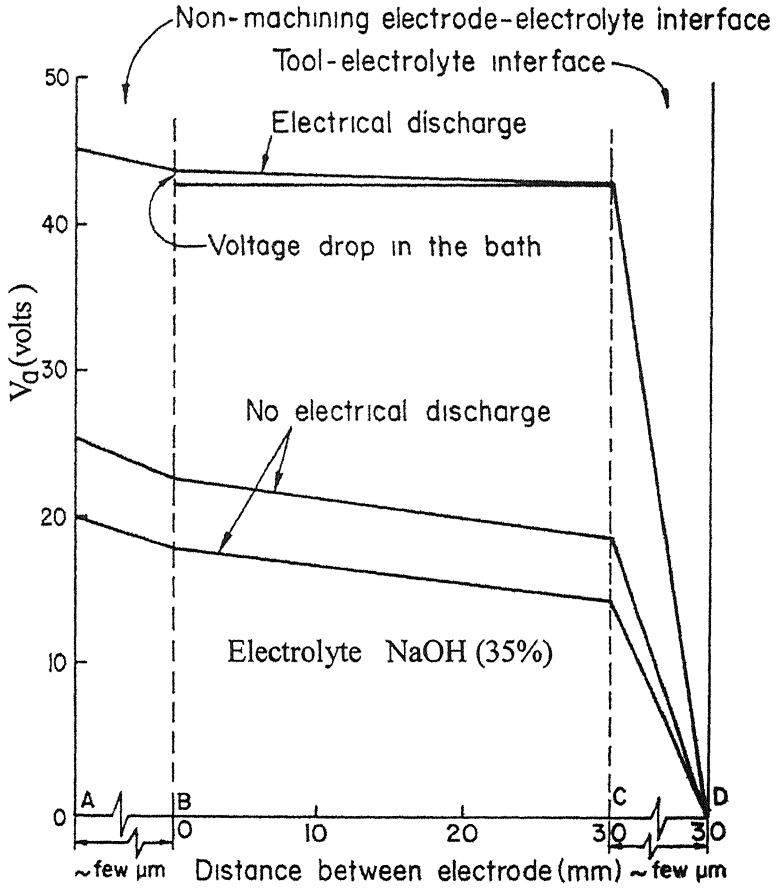

Fig 1 2 Distribution of voltage drop in ECSM bath [2]

electrolyte He explained the reason for limiting machined depth characteristic as a result of decrease in the potential available between tool and electrolyte (across the insulating layer of gas and vapour bubbles) with increase in machined depth He also observed upward shifting of the sparking zone when tool penetrated into work-piece

In 1991 Jain et al [3] used traveling wire electrochemical spark machining (TW -ECSM) for cutting thick sheet of composite material They have reported an increase in MRR, TWR, and over cut with an increase in voltage and electrolyte concentration (NaOH, up to 22.5% by weight) Beyond this concentration of NaOH, above responses decrease because specific conductance of NaOH decreases beyond 22 5% concentration by weight. The effects of artificially generated bubbles have also been studied Introduction of artificial bubbles into the machining zone reduces MRR Because of the larger size of the artificial bubbles, discharge does not take place across some bubbles by existing potential gradient, but it improves the machining accuracy (or lower average diametral overcut) Results are shown in Fig 1 3

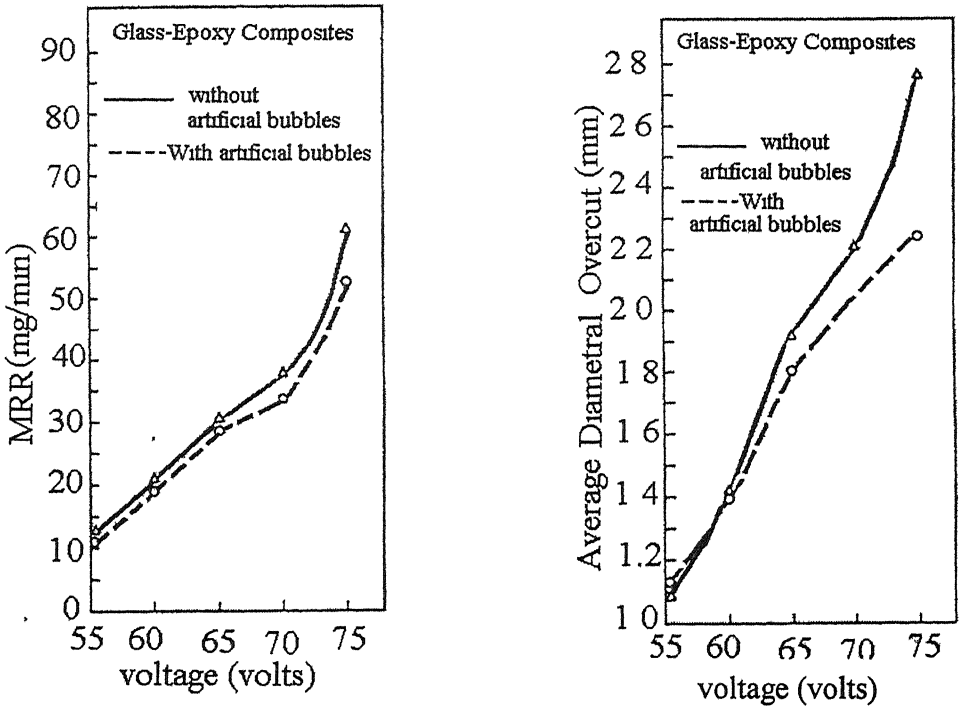

Fig 1 3 Effect of artificial bubbles on MRR and overcut [3]

In 1995, Raghuram et al [4] studied the effect of various circuit parameters on the electrolytes in electrochemical discharge phenomenon They used various types of circuit configuration like rectified dc, rectified dc with a series of inductor, etc and concluded that the external circuit parameters have definite influence on discharge characteristics

In 1996, Singh et al [5] reported the findings related to TW-ECSM experiments on partially electrically conductive materials viz, piezo-electric ceramics (PZT) and carbon fiber epoxy composites They concluded that further investigations related to the effect of machining parameters on the surface integrity are required before this process becomes commercially viable Experiments were performed [6] on ceramics with different tool kinematics like stationary tool, rotating tool with or with out electrolyte flow, tool with orbital rotation, and controlled feeding of the workpiece By using trepanning action and controlled feed to the workpiece, MRR and limited drilling depth can be substantially increased (Fig 1 4)

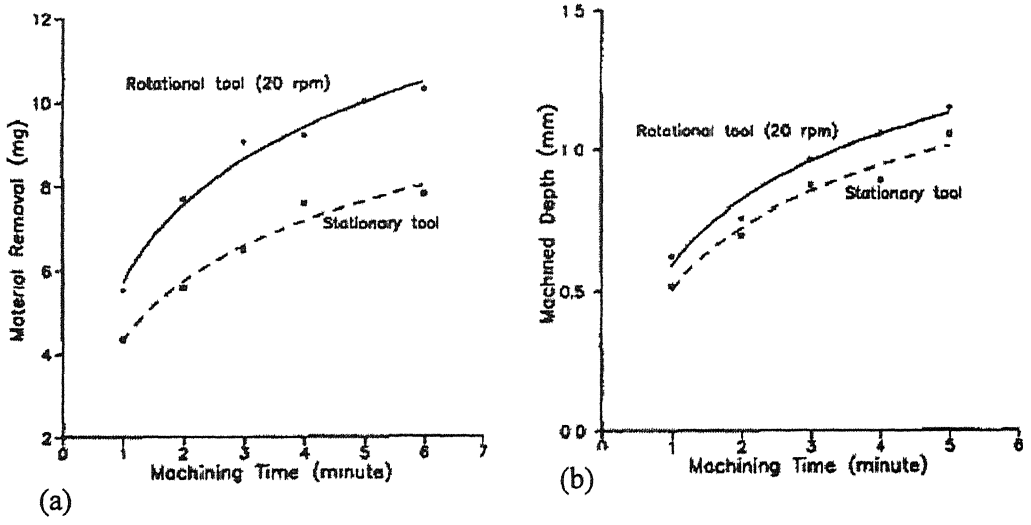

Fig.1 4 Improved MRR and machined depth by trepanning action [8]

In 1997, Basak et al [7] did the theoretical analysis of the mechanism of spark generation They concluded that the mechanism of sparking in ECSM process is similar to switching off phenomenon in electrical circuit He also reported that MRR can be increased by 200% by introducing external inductance to the circuit (Fig 1 5) Singh [8] concluded material removal in alumina takes place due to crack propagation and etching of grain boundaries in heated electrolyte Jain et al [9] proposed the application of "valve theory" to the spark generation in ECSM process From the V-I characteristics in a discharge tube they concluded that sparking in ECSM process is similar to the arc discharge that occurs in discharge tube Limited machined depth in drilling operation can be explained by plotting the isotherms There is the possibility of no sparking near some of the unmelted materials (Fig 1 6) that causes limited machining depth in ECSM process

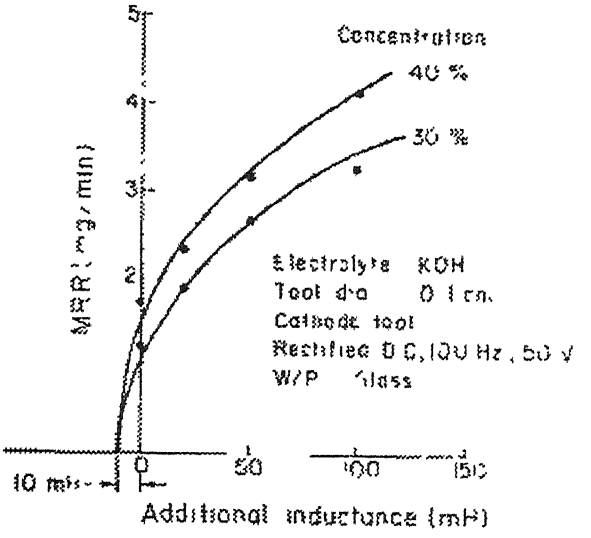

Fig 1 5 Improved MRR by additional inductance [7]

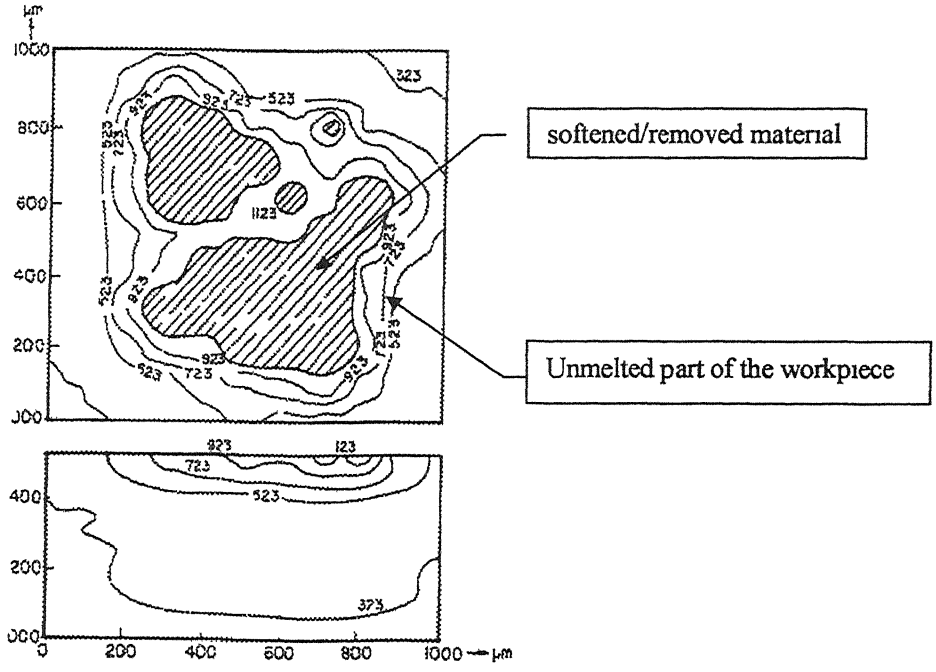

Fig 1 6 Intermediate isotherms for soda lime glass after 10 sparks at supply voltage of 40 V [9]

In 1999, Dolol et al [10] conducted experiments on alumina They concluded that the most effective parametric combinations for moderately higher machining rate and dimensional accuracy are 80 V and 25 % NaOH concentration They reported tool tip geometry plays important role for controlled spark generation Overcut value for taper side wall-flat front tool (Fig 1 7(ii)), is much less compared to straight side wall-flat front tool (Fig 1 7(i)) and taper side-curved front tool tip (Fig 1 7(iii)) due to occurrence of concentrated sparking at the tool tip Dolol et al [11] used Taguchi method for optimizing the machining parameters in ECSM process

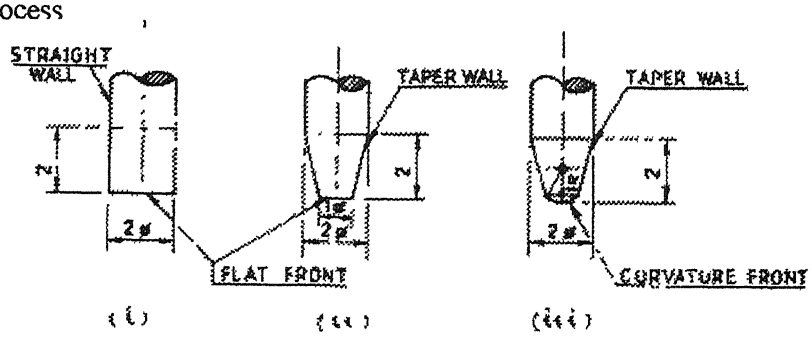

Fig 1 7 Different geometrical shapes of the tool tip (dimensions mm) [10]

In 2000, Chak [12] improved machined depth on alumina and quartz by using high voltage and high temperature of NaOH solution

In 2002, Jain et al [13] used rotating tool having impregnated abrasive particles (ECSM+GRINDING→ ECSG), and found that MRR and machined depth increase because of combined effect of thermal erosion and grinding operation (Fig 1 8) Kulkarni et al. [14] studied the variation of current with respect to time in ECSM process They also observed the geometry of single discharge affected zone, is circular in nature and diameter of about 300μm A high electric field of the order of 10^7 V/m is generated across the bubbles on the cathode tip and an arc discharge [9] takes place

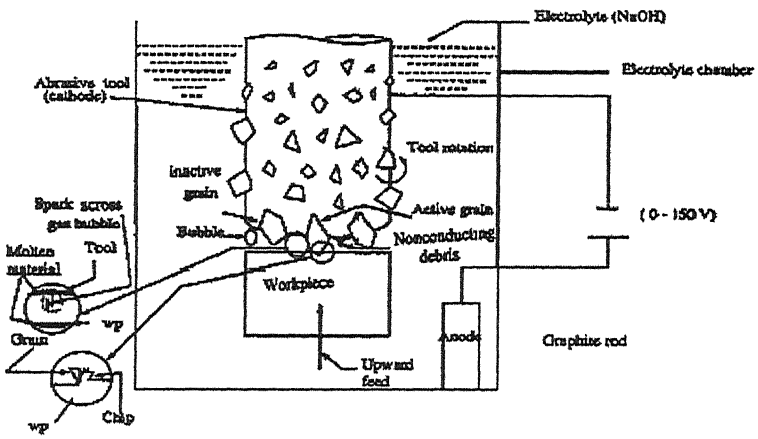

Fig 1 8 Schematic diagram of electrochemical spark grinding set-up [13]

1.3 Objective of present work

Slicing of quartz plate by electrochemical spark sinking operation has been attempted first time in this work Literature survey reveals even though substantial amount of experimental work-has been done, but no data is available on the surface finish characteristics of the machined profile in ECSM process Preliminary experiments also show that if we reverse the

polarity (tool is positive) MRR is higher than direct polarity (tool is negative), even though visually observed spark intensity seems to be lower for reverse polarity Therefore, ECSM process can be classified as electrochemical spark machining with direct polarity (ECSMWDP) and electrochemical spark machining with reverse polarity (ECSMWRP) Hence, the following objectives of the present work have been set

1 Application of ECSM process for cutting of quartz plate by controlled feeding of workpiece
2 Measurement of surface finish of the machined profile in ECSM process
3 To study the basic mechanism of material removal in ECSMWRP while machining quartz
4 To study the feasibility of machining simultaneously at both electrodes (ECSMWDP and ECSMWRP)

Chapter 2

EXPERIMENTAL SET-UP

Experimental set-up consists of work holding and work feed mechanism, tool and tool holder, mechanical switch, stepper motor controller, temperature controller and power supply

2.1 Work holding and feeding mechanism

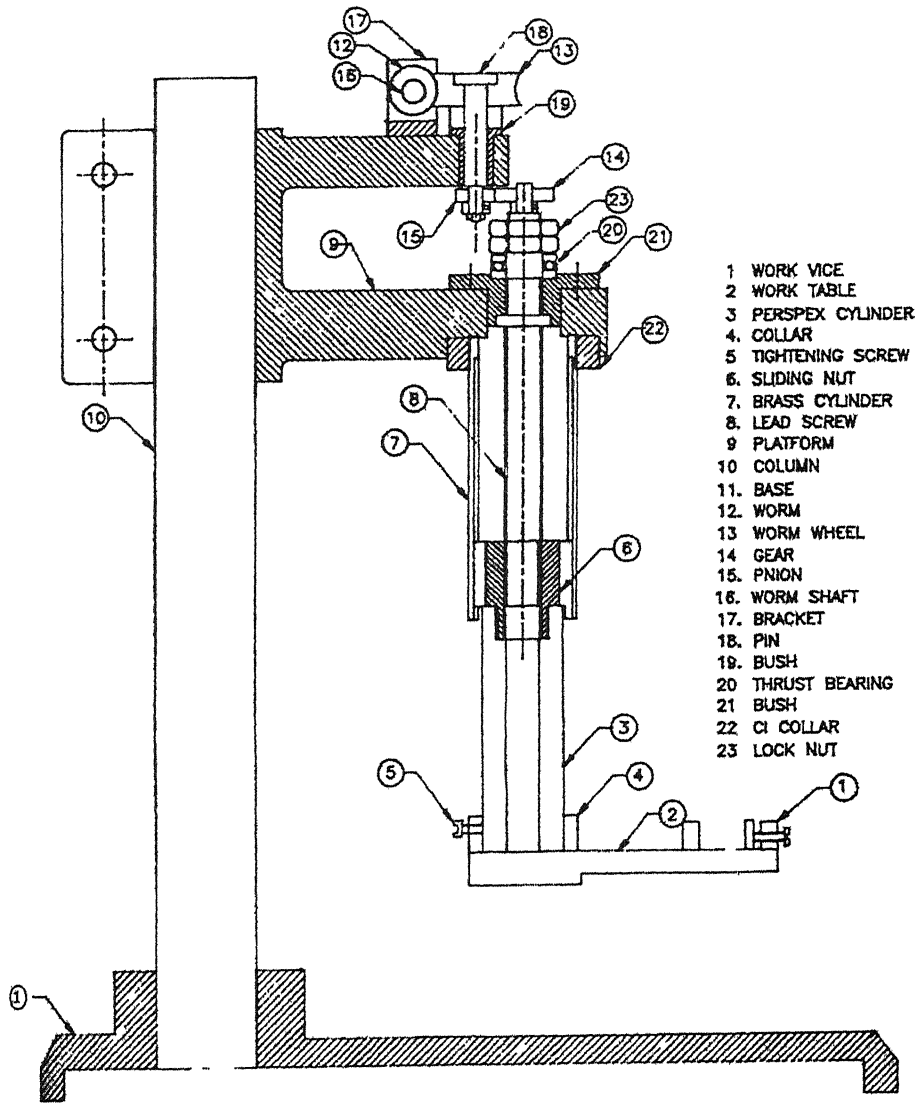

Fig 2 1 Work feed and holding mechanism [15]

Experimental set-up designed and fabricated by Gautam [15] was used for the experiments Work-piece feeding mechanism is shown in Fig 2 1 Feed rate is very low in ECSM process Smooth rotation of motor (12V, 20 kg-cm) was obtained by using high reduction ratio between motor and lead screw (pitch 1 45 mm) Motor is directly connected to worm and worm wheel (40 1) Worm wheel is connected to lead screw by spur gears (1 1) A vice is mounted on the work table for holding the work-piece By rotating of the lead screw upward or downward movement is given to worktable

2.2 Tool and Tool holder

Copper was used as tool material Tool geometry plays an important role for effective spark generation Requirements for tool design are, it should be able to cut at fast rate and produce good quality surface Tool should have sufficient strength to withstand mechanical forces Spark intensity is more at the sharp corners of the tool because of high charge density Therefore, sharp edged tool was used for cutting operation It produces less overcut and high penetration rate compared to flat tool Tool size, 4X0 5X20 mm (Fig 2 2) has been selected so that it is able to cut for sufficient depth Fig 2 3 shows the details of the tool and tool holding assembly

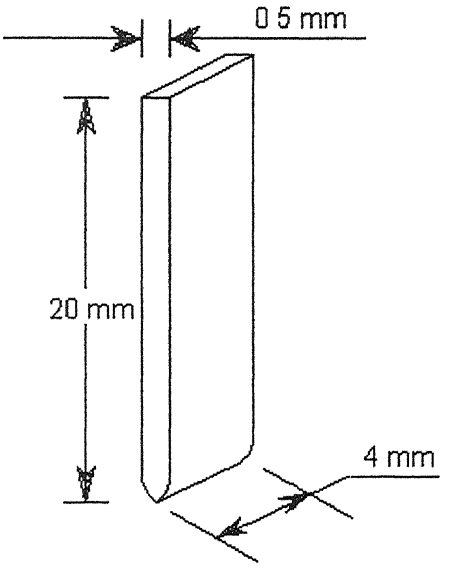

Fig 2 2 Tool used for experiments

2.3 Mechanical switch

For efficient machining, a gap between tool and work-piece is essential so that electrolyte is always available between the bottom of the tool and workpiece for generating sparks As work-piece is electrically nonconductive, gap voltage or gap current sensing servomechanism for maintaining the gap between tool and work-piece can't be used A mechanical switch has been designed for sensing the contact between work-piece and tool Mechanical switch consists of an adjusting screw and a copper plate (Fig 2 3) They are connected to status port of PC printer port When feed rate is higher than machining rate, tool touches the work-piece and it pushes tool holder assembly upwards Therefore copper plate also starts moving in upward direction and it strikes the adjusting screw Value of status port is changed from 127 to 255 and motor starts rotating in a reverse direction Thus work table is lowered down for creating the gap between tool and work-piece The micro gap between copper plate and screw can be adjusted by screwing on or screwing off the screw

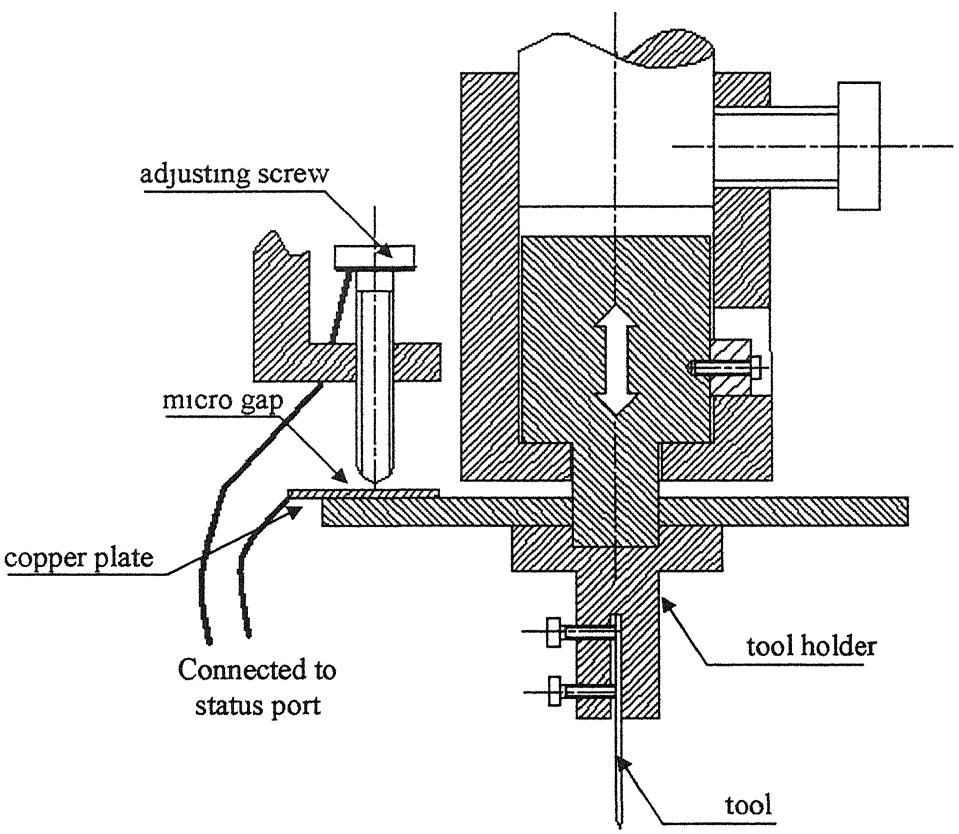

Fig 2 3 Tool holding and mechanical switch assembly

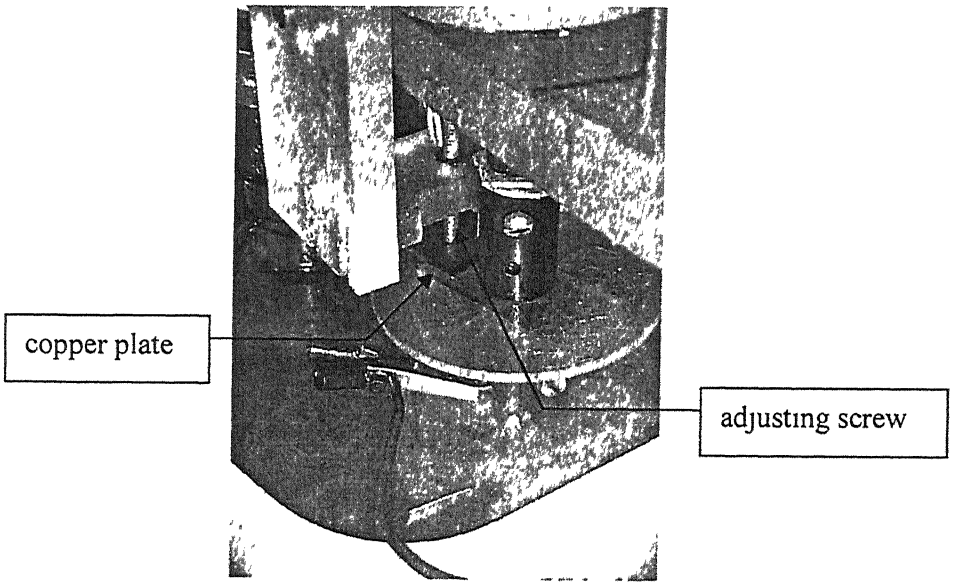

Fig 2 4 Mechanical switch

2.4 Stepper motor controller

Schematic diagram of the stepper motor controller used in experiment is shown in Fig 2 5 Stepper motor can be precisely controlled by using PC Printer Port Each printer consists of

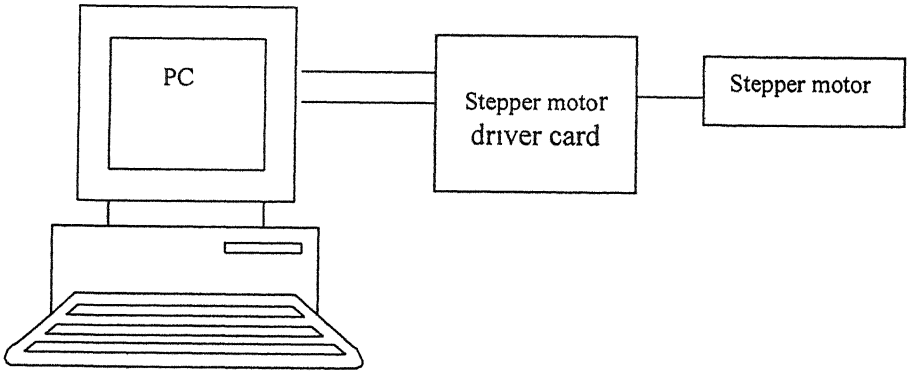

Fig 2 5 Stepper motor control diagram

three port addresses, data, status and control port These addresses are in sequential order That is data port address 0x0378, the corresponding status port is at 0x0379 and the control port is at 0x037a Fig 2 6 and Fig 2 7 [16] illustrate the pin assignments on 25 pin connector and bit assignments on three ports Data ports were used to generate the direction bits and clock signals at required frequency Status port, pin no 13 was used to control the direction of rotation of the motor Default value of the status port is 127 When we make pin no 13 ground, value of status port becomes 255. Therefore, if shorting occurs between adjusting screw and copper plate of mechanical switch because of higher feed rate, value of the status port becomes 255 At that time value of the direction bit changes from 0 to 1 and motor starts rotating in reverse direction for 15 rotations to create required gap between tool and work-piece In the mean time the switch is disconnected and value of the status port is now 127 After completing the reverse rotations, motor again starts rotating in forward direction A software program in C has been written for controlling the stepper motor by PC printer port (Appendix-1) Machining time and penetration depth were also recorded by the program Flow chart of the program is shown in Fig 2 8

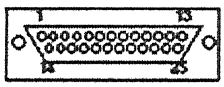

View is looking at
Connector side of
DB-25 Male Connector

Pin	Description	
1	Strobe	PC Output
2	Data 0	PC Output
3	Data 1	PC Output
4	Data 2	PC Output
5	Data 3	PC Output
6	Data 4	PC Output
7	Data 5	PC Output
8	Data 6	PC Output
9	Data 7	PC Output
10	ACK	PC Input
11	Busy	PC Input
12	Paper Empty	PC Input
13	Select	PC Input
14	Auto Feed	PC Output
15	Error	PC Input
16	Initialize Printer	PC Output
17	Select Input	PC Output

Pin Assignments

Note 8 Data Outputs
4 Misc Other Outputs

5 Data Inputs

Note Pins 18-25 are
Ground

Fig 2 6 Pin assignments for PC printer port

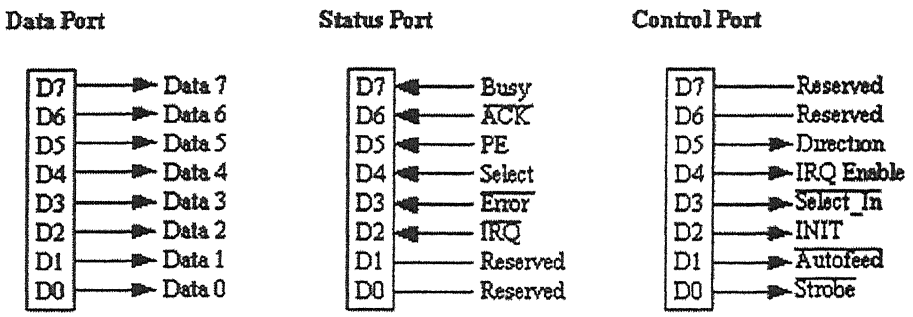

Fig 2 7 Port assignments

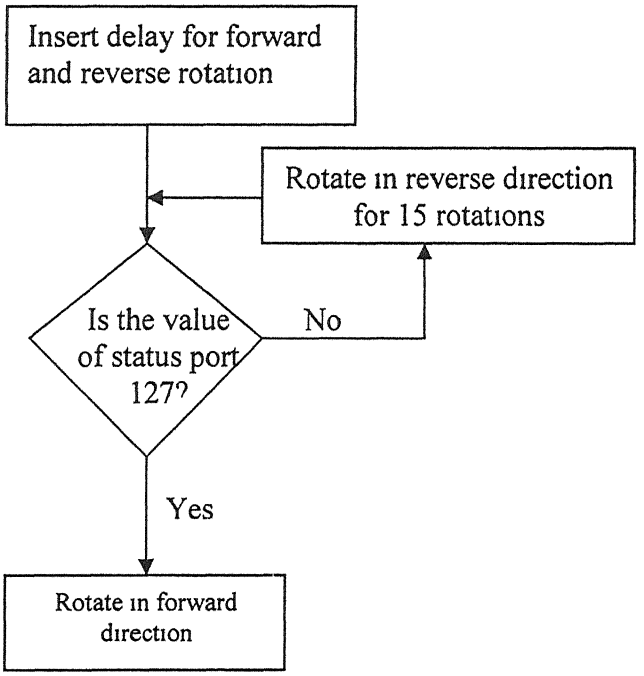

Fig 2 8 Flow chart of the program

2.5 Temperature controller

Conductivity of electrolyte is highly sensitive to temperature During the experiment to maintain constant electrolyte temperature between anode and cathode a temperature controller has been designed (Fig 2 9) A Contact thermometer was kept between electrodes Electrolyte was heated by immersion heater Power goes to heater through a 6 V relay Voltage at resistance variac was set to 140 V for slow heating of electrolyte Required temperature level can be set in contact thermometer Temperature of electrolyte rises because of heating by immersion heater When temperature reaches to set value circuit inside the contact thermometer is completed and electromagnet inside the relay is activated It cuts off power supply to the heater and heater is switched off Temperature of the electrolyte starts decreasing because of lower ambient temperature Mercury level inside the thermometer drops and circuit inside the thermometer is disconnected Therefore electromagnet inside the relay is demagnetized and power supply again goes to heater and heater is switched on

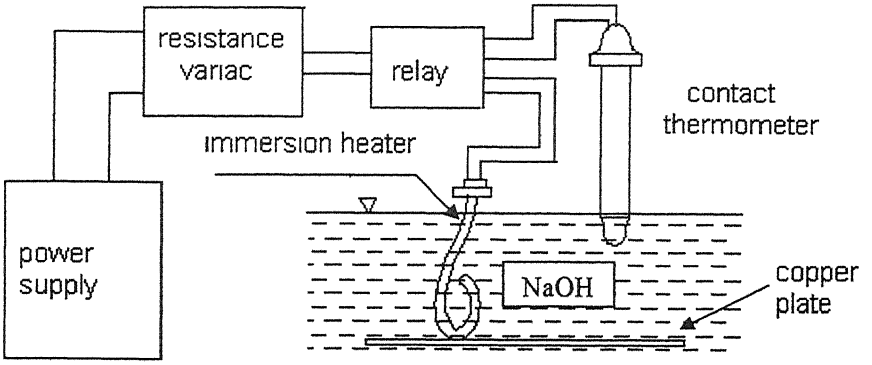

Fig 2 9 Temperature controller

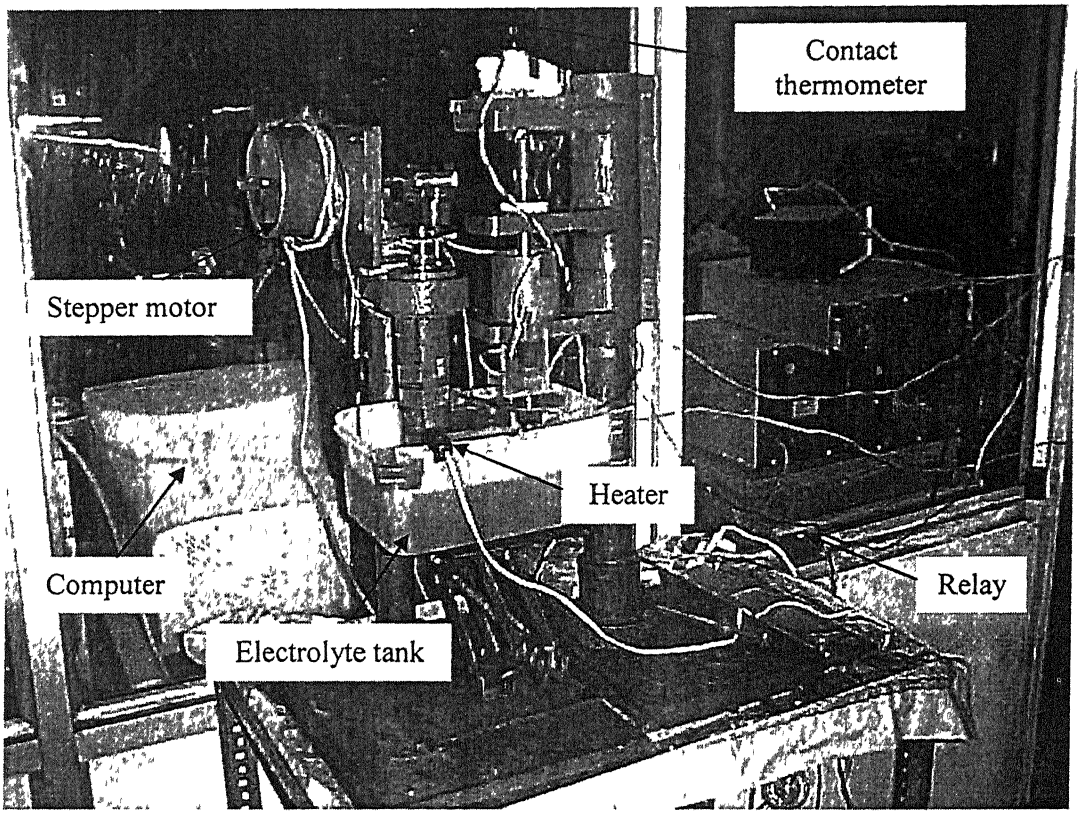

Fig 2 10 Experimental set-up used for experiment

2.6 Experimentation

Conductivity of the electrolyte was measured by conductivity meter. Initially work-piece was touched with tool tip and gap between adjusting screw and copper plate was measured by counting the number of rotations of the motor required to short the switch Gap between adjusting screw and copper plate can be adjusted by rotating the screw After adjusting the gap, motor was rotated in reverse direction for creating the gap between tool tip and work-piece Machining was started with a constant gap between tool and work-piece Tip of the tool was 2-3 mm dipped into electrolyte. Level of the electrolyte was maintained by

constantly supplying electrolyte into the tank A constant feed rate was provided to the work-piece If feed rate is higher than material removal rate, tool tip touches the work-piece and force is exerted to tool which lifts the tool holding assembly This movement shorts the mechanical switch and motor starts rotating in reverse direction Work table is lowered down to create the gap between tool and work-piece When motor rotates in reverse direction power supply to the electrodes was switched off to stop the overcut during that period After creating the gap motor starts rotating in forward direction and the voltage is again applied between the electrodes to start cutting Number of rotations of the motor was counted by the program Machining depth was automatically calculated by subtracting the total reverse number of rotations from the total number of forward rotations Machining time was calculated by multiplying total number of steps with time required per step

Thickness of work-piece chosen was of 2 mm So that, reaction products are easily removed from machining zone by cavitation, diffusion, flow of ions etc and does not impose the condition of limited machined depth Cutting conditions during experiments are given in Table 2 1

Table 2 1 Machining conditions
Work-piece material = Quartz
Work-piece thickness = 1 9 to 2 1 mm
Electrode material = Copper
In ECSMWDP,
Cathode size = 4X0 5X20 mm
Anode size = 110 X 2 X 50 mm
In ECSMWRP,
Anode size = 4X0 5X20 mm
Cathode size = 110 X 2 X 50 mm
Electrolyte = Sodium hydroxide (NaOH)
Inter-electrode gap = 50 mm
Electrolyte concentration = 10 to 22% by wt
Specific electrolyte conductivity = 369 to 448 mmho/cm
Voltage range = 60 to 84 V
Electrolyte temperature= 40 ^{0}C
Feed rate to work-piece = 0 339 mm/min
Initial gap between tool and work-piece =0 4 mm
Gap between adjusting screw and copper plate = 127 to 145 μm
Machined depth ≥ 6 66 mm
Electrolyte used for each experiment = 3 liters

2.7 Design of experiments

Planning for experimentation is required before conducting the experiments It involves selection of machining conditions, planning for experiments, conducting the experiments, etc From the literature survey, it is concluded that voltage and electrolyte concentration are

the most significant parameters for material removal in ECSM process Therefore only voltage and electrolyte concentration have been selected as process variables Overcut, surface finish, penetration rate and tool wear have been selected as responses for the experimentation

The general form of a quadratic (second order) polynomial is illustrated by the equation,

$$y = \beta_0 + \sum_{i=1}^{k} \beta_{ii} x_i^2 + \sum_{i=1}^{k} \beta_{ii} x_{ii}^2 + \sum_{i<j} \beta_{ij} x_i x_j$$

Where y is response, k is total no of variables, x_i is i^{th} quantitative variable and β_0, β_i, etc are regression coefficients

2 7.1 Central composite rotatable design (CCRD)

CCRD is the most popular class of design is used for fitting quadratic model Central composite rotatable design consists of 2^k factorial (or fractional factorial) with n_F runs, 2k axial or star runs and n_c center runs [17, 18]

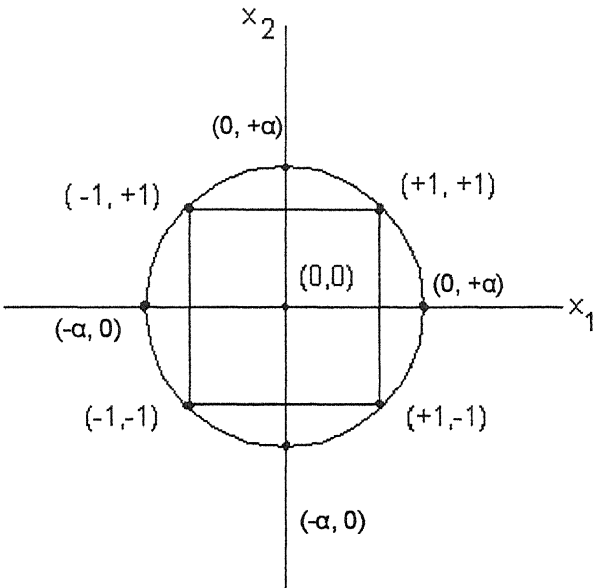

Fig 2 11 Central composite design for two factors

From Fig 2 11, for two variables n_f runs are (-1,-1), (1,-1), (-1, 1), (1, 1), axial runs are (-α, 0), (α, 0), (0,-α), (0,α) and center run is (0, 0) Where $\alpha = (n_F)^{1/4}$ and no of center runs usually $3 \leq n_c \leq 5$

According to CCRD whole range for voltage and electrolyte was divided into five levels For two factors,

$n_f = 2^2 = 4$

$\alpha = (n_F)^{1/4} = 1.414$

Actual value = mean value + ((mean value- minimum value)* coded value)/1 414

Coded value	Actual value	
	Voltage (V)	Electrolyte concentration (% by wt)
-1 414	60	10
-1	63 5	11 76
0	72	16
1	80 5	20 24
1 414	84	22

Chapter 3

FUNDAMENTALS OF ECSMWRP

Experiments were conducted by using one small and one large electrode Small electrode was used as tool Small electrode was made as cathode (ECSMWDP) or anode (ECSMWRP), by changing the polarity By electrochemical reactions, at cathode hydrogen gas and at anode, oxygen gas is liberated Boiling of electrolyte solution near small electrode occurs by the heating of electrolyte due to high resistance to current flow Therefore, electrically non-conductive layer of gas-vapour mixture is formed in both cases (ECSMWDP and ECSMWRP) and it shields small electrode Sparking occurs between tool and electrolyte because of the breakdown of the insulating layer due to high potential gradient across the insulating layer Experimental observations reveal that spark intensity is higher at small electrode, when it is cathode (ECSMWDP) compared to when it is anode (ECSMWRP) But, material removal rate (penetration rate and overcut) and tool wear rate is higher in ECSMWRP compared to ECSMWDP (Table 3 1) Therefore, it seems that material removal in ECSMWRP is not only by melting and vaporization of workpiece material by the heat generated due to sparking Deep crater formed in anode at anode-workpiece interface (Fig 4 7) leads to conclude that some chemical reaction is occurring at anode-workpiece interface It has also been observed in ECSMWRP that spark intensity is more at zone-b compared to zone-a (Fig 3 1) This is due to higher resistance to current flow in small gap between tool and workpiece at zone-b compared to zone-a In this chapter, possible chemical reactions that can occur at anode electrode interface have been proposed from basic electrochemistry Chemical analysis of reaction products have also been carried out

Table 3 1 Comparison between ECSMWDP and ECSMWRP
(Voltage 72, Electrolyte concentration 10% by wt)

Tool	Machining time (min)	Work-piece		Tool		Over-cut (mm)	Machi-ned depth (mm)	MRR (mg/min)	Tool wear rate (mg/min)	Penetra-tion rate (mm/min)
		Initial Wt (mg)	final wt (mg)	initial wt	final wt					
+ ve (ECSMWRP)	23 724	0 456	0 421	0 429	0 416	0 175	6 66	1 47	0 548	> 0 339
-ve (ECSMWDP)	59 310	0 909	0 876	0 411	0 408	0 108	7 175	0 343	0 050	~ 0 120

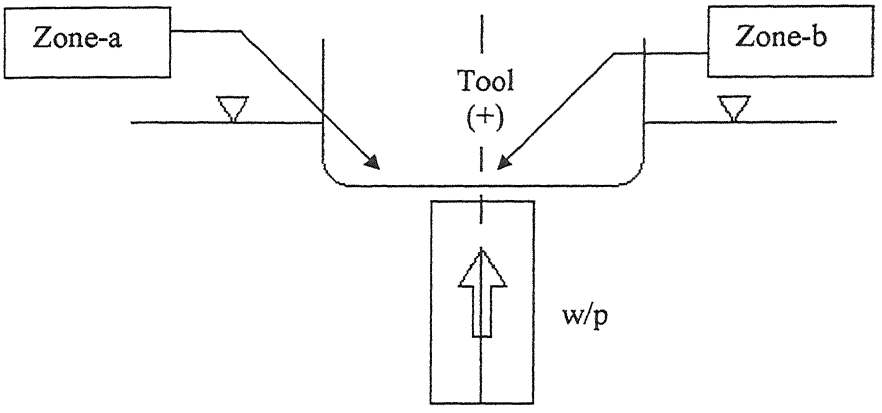

Fig 3 1 Different zones at tool tip

3.1 Electrochemistry for NaOH electrolyte and copper electrodes

Schematic diagram of an electrolytic cell of NaOH solution and copper electrode is shown in Fig 3 2 External potential is applied between the electrodes In the external circuit, electrons move towards the cathode-electrolyte interface, and go to the solution At anode electrolyte interface equal number of electrons is discharged from solution to the anode Thus, current flows through the external circuit Electrochemical reactions that occur at the electrode electrolyte interface continuously supply electrons from cathode to solution and solution to anode Which type of reactions occur, depends on the characteristics of electrodes, electrolyte and applied voltage [19, 20, 21]

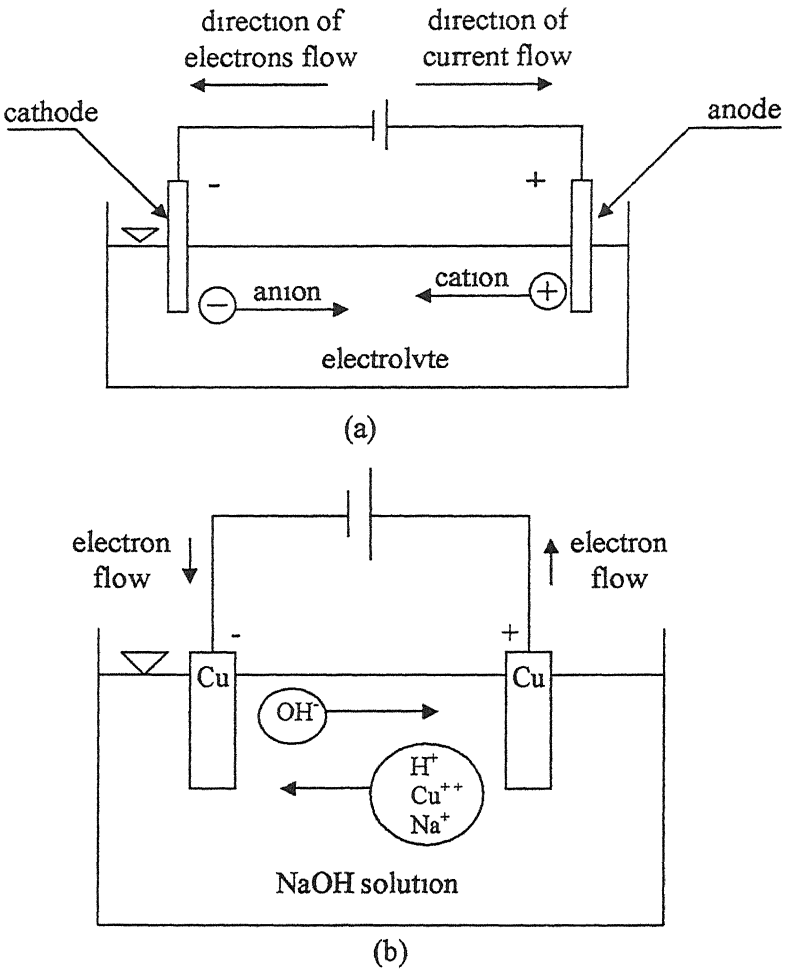

Fig 3 2 Schematic diagram of the flow of electrons and ions in electrolytic cell [(a) General representation of an electrolytic cell, (b) Electrolytic cell of NaOH solution and copper electrodes]

Reactions at anode electrolyte interface:

The electrochemical reactions at anode electrolyte interface cause generation of oxygen gas and dissolution of anode

$Cu \rightarrow Cu^{++} + 2e^-$

$2H_2O \rightarrow O_2\uparrow + 4H^+ + 4e^-$

Here, oxygen bubbles and vapour bubbles generated by boiling of electrolyte due to high resistance to current flow forms the electrically non-conductive layer on anode surface

Reactions at Cathode and electrolyte interface:

The electrochemical reactions at cathode electrolyte interface cause evolution of hydrogen gas and deposition of copper

$Cu^{++} + 2e^- \rightarrow Cu$

$2H^+ + 2e^- \rightarrow H_2\uparrow$

$Na^+ + e^- \rightarrow Na$

$2Na + 2H_2O \rightarrow 2NaOH + H_2\uparrow$

$2H_2O + 2e^- \rightarrow H_2\uparrow + 2OH^-$

Here, hydrogen bubbles and vapor bubbles generated by boiling of electrolyte forms the insulating layer on anode surface

3.2 Dissolution of quartz

Schematic diagram of machining of quartz by ECSMWRP is shown in Fig 4.3 Reduction of silicon dioxide (SiO_2) occurs due to high electromotive force generated by high potential gradient A small gap between anode and work-piece also generates high resistance Sparking occurs due to high charge density and high resistance to current flow through anode-workpiece interface Heat generated by sparking accelerates the reduction process Freshly formed silicon is highly active and it is re-oxidized by fresh oxygen gas evolved at anode This newly precipitated SiO_2 is highly amorphous in nature and prone to chemical reactions [22] It reacts with sodium hydroxide to form sodium silicate and so dissolves into the NaOH solution and also forms copper silicate The reactions are as follows,

SiO_2 (Quartz) $+ 4e^- + 4H^+ \rightarrow Si + 2H_2O$ (or $SiO_2 + 4H(2H_2) \rightarrow Si + 2H_2O$)

$Si + O_2 \rightarrow SiO_2$

SiO_2 (amorphous) $+ 2OH^- \rightarrow SiO_3^{--} + H_2O$

$SiO_2 + 4OH^- \rightarrow SiO_4^{4-} + 2H_2O$

$2Na^+ + SiO_3^{--} \rightarrow Na_2SiO_3$

$4Na^+ + SiO_4^{4-} \rightarrow Na_4SiO_4$

$Cu^{++} + SiO_3^{--} \rightarrow CuSiO_3$

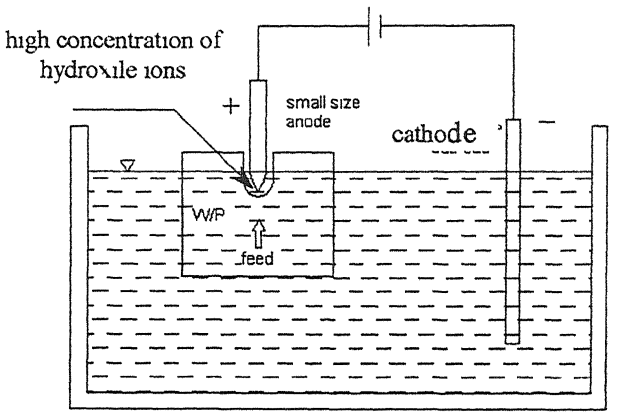

Fig 3 3 Machining of quartz by ECSMWRP

3.3 Reason for Tool shape deterioration

Tool wear rate in anode-workpiece interface is much higher Therefore a deep crater is formed at interface zone (Figs 3 4, and 4 5) From anode, copper is transferred to solution as copper ion ($Cu \rightarrow Cu^{++} + 2e^-$) which results in tool wear Copper ions react with hydroxyl ions to form copper hydroxide ($Cu^{++} + OH^- \rightarrow Cu(OH)_2$) At interface zone, copper ions react with silicate ions to form copper silicate ($Cu^{2+} + SiO_3^{2-} \rightarrow CuSiO_3$) Therefore, at interface zone (zone-b, Fig 3 1), copper ions are transferred from anode into solution at faster rate compared to zone-b because both the reactions take place at interface zone This causes the high rate of formation of copper ions, i e , high rate of dissolution of copper from anode at interface zone Small gap between anode and workpiece at interface zone generates high resistance to current flow Therefore, sparking is more at interface zone compared to zone-b This also causes more tool wear at interface zone

$Cu \rightarrow Cu^{++} + 2e^-$

$Cu^{++} + OH^- \rightarrow Cu(OH)_2$

$Cu^{++} + SiO_3^{--} \rightarrow CuSiO_3$

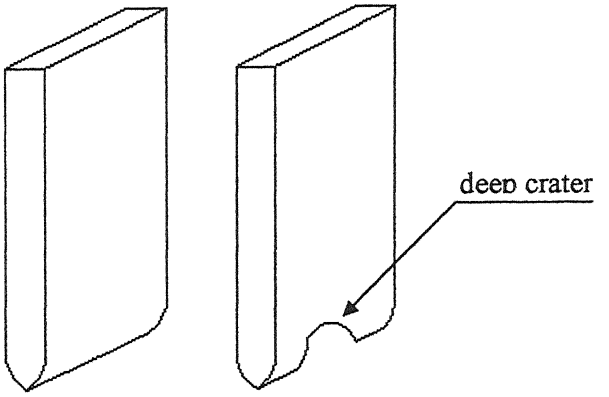

(a) before machining (b) after machining

Fig 3 4 Tool shape

3.4 Chemical analysis

After cutting quartz plate by ECSMWRP, NaOH solution would contain silicon dioxide (SiO_2), sodium silicate (Na_2SiO_3), copper silicate ($CuSiO_3$), copper hydroxide (Cu $(OH)_2$) and oxides of copper (CuO) It has been experimentally observed that, Copper silicate in NaOH medium forms precipitate of copper oxide and silica parts goes to solution in the form of $[Cu(OH)_2(SiO_3)_x]^n$ ($CuSiO_3$ + NaOH $\rightarrow [Cu(OH)_2(SiO_3)_x]^n$ + CuO) Standard copper silicate was prepared from sodium silicate and copper chloride ($Na_2SiO_3 + CuCl_2 \rightarrow CuSiO_3$ + 2 NaCl) Copper silicate was put into water and sodium hydroxide solution in two separate test tubes In water, copper silicate precipitates, but in NaOH solution black of copper oxide (CuO) precipitates and a light blue solution was formed (Fig 3 5) This indicates, in alkaline medium from copper silicate, silicate ion goes into solution as complex compound of copper ($[Cu(OH)_2(SiO_3)_x]^n$) that makes light blue solution Therefore if the residues are separated from NaOH solution after cutting quartz, solution would contain sodium silicate and complex compound of copper silicate that are soluble in NaOH solution

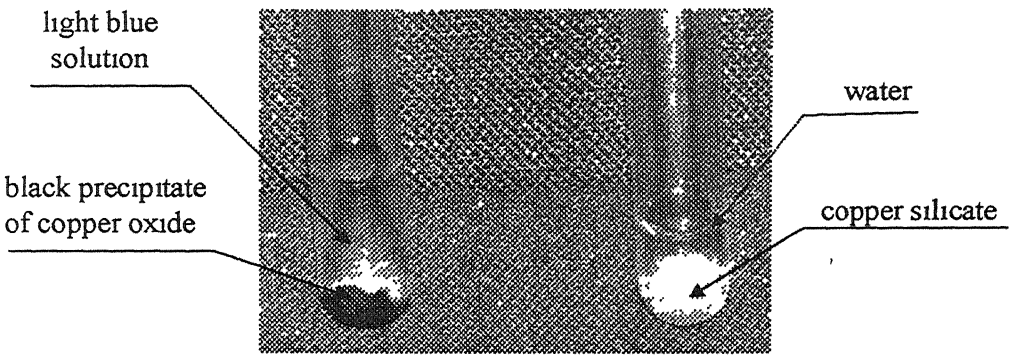

(a) copper silicate in NaOH solution (b) copper silicate in water

Fig 3 5 Copper silicate in alkaline and neutral solution

After conducting experiments, NaOH solution was filtered Thus, the precipitate was separated from solution After that the solution was digested on water bath and found that gelatinous silica floats into solution ($Na_2SiO_3 + 4H_2O \rightarrow H_2SiO_3 + 2NaOH$) By centrifuging the solution, white mass was precipitated It was dried in oven and turned into whitish-pink colored solid It indicates the presence of copper compound into centrifugate White-pink colored solid was treated with concentrated HCl It forms a yellowish solution and white flocculating solid White flocculating solid is silicic acid (H_2SiO_3), which is not dissolved in HCl Thus, it confirms the dissolution of quartz into NaOH solution Yellowish solution was separated and NH_4OH was added into it It turns into light blue solution confirming the presence of Cu^{++} ion This copper ion comes from copper silicate, by the formation of soluble complex compound into NaOH solution Flow chart of the chemical analysis of the solution has shown in Fig 3 6

Therefore, it can be concluded that in ECSMWRP quartz dissolves into NaOH solution by chemical reactions Dissolution of quartz may be in the form of sodium silicate and copper silicate

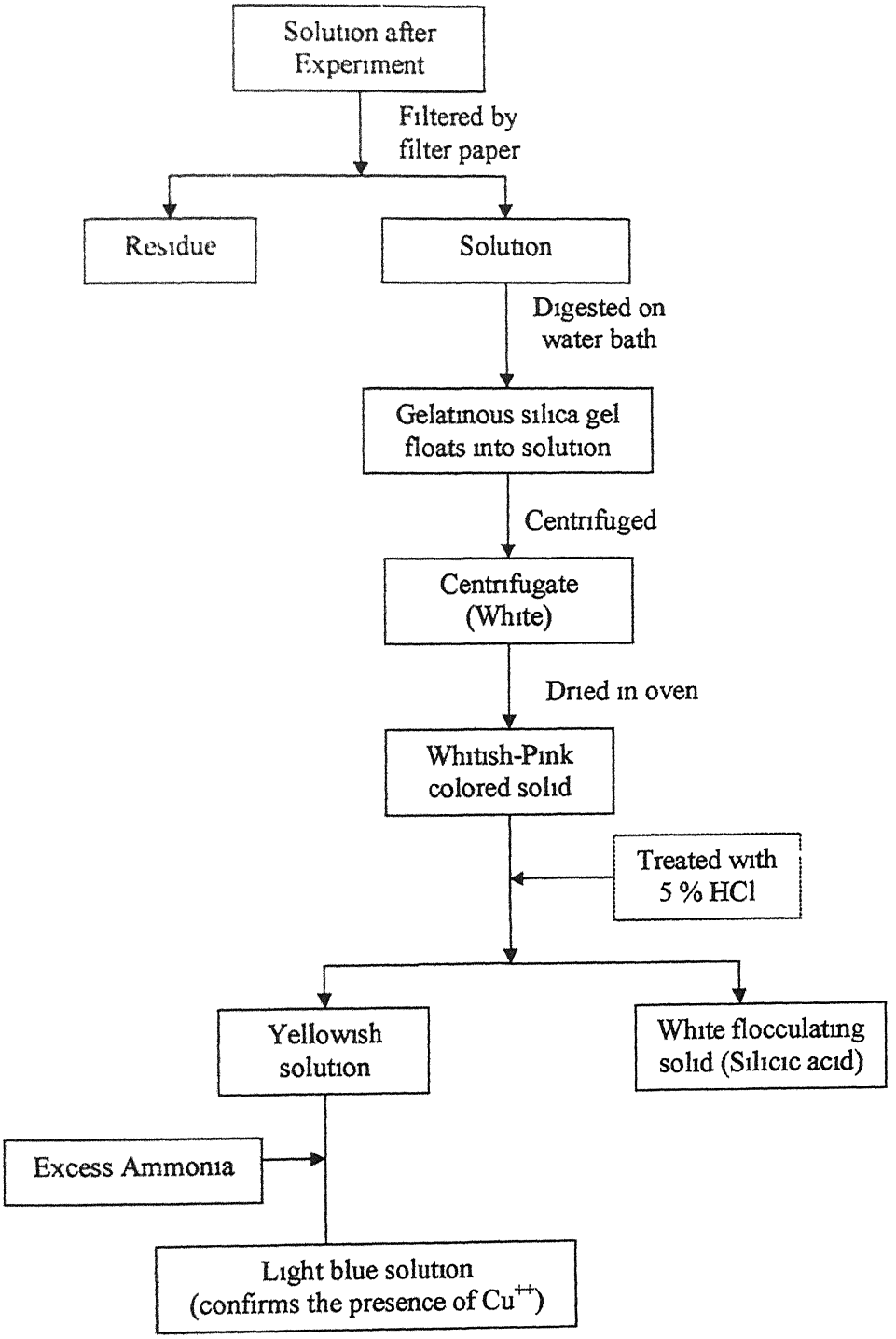

Fig 3 6 Flow chart for chemical analysis of solution after experiment

Chapter 4

EXPERIMENTAL RESULTS AND DISCUSSIONS

During experiments, quartz plate was cut for a depth of more than 6 66 mm (Fig 4 1) Experiments were conducted for both direct polarity and reverse polarity under same experimental conditions. After experiments, overcut of the machined cavity and surface roughness of the machined surface, tool wear and penetration rate were measured for the process performances evaluation

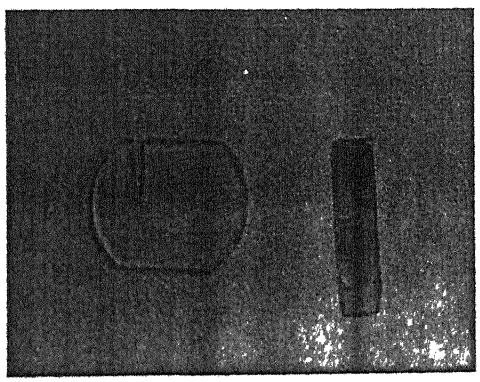

(a)

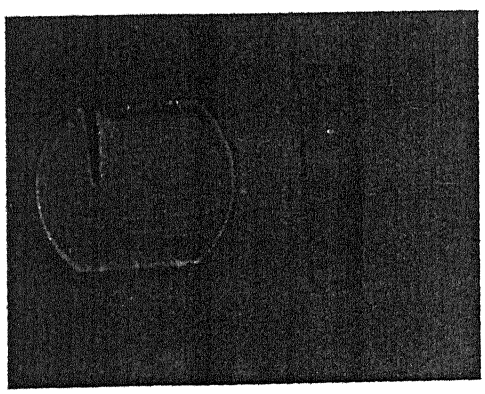

(b)

Fig 4 1 Work-pieces and tool after experiment cutting [(a) Tool and workpiece after cutting by ECSMWDP, (b) Tool and workpiece after cutting by ECSMWRP

4.1 Penetration rate

If linear material removal material rate (or penetration rate) is more compared to feed rate, tool reversal will not occur. However, in ECSMWDP frequent tool reversal was occurring because of low penetration rate (Table 3.1). But in ECSMWRP tool reversal was less because of higher penetration rate and higher tool wear rate. Comparison of feed rate and penetration rate obtained for ECSMWRP at different cutting conditions is shown in Table 4.1. Except for experiment no. 3 & 5, tool reversal is negligible. It is so because penetration rate in ECSMWRP is more than the feed rate for most of the experiments conducted at different voltage and electrolyte concentration. It has been experimentally observed that the depth of tool tip dipped into the electrolyte plays an important role in determining the penetration rate in ECSMWRP process. If tool tip dipped into the electrolyte is very less in ECSMWRP, penetration rate deteriorates. It is difficult to maintain the narrow range of 2-3 mm of depth to which the tool tip is dipped into the electrolyte because of the surface tension of liquid, and continuous tool wear, sparking at machining zone and cavitation in machining zone.

Table 4.1 Comparison between federate and penetration rate in ECSMWRP

Exp No	Voltage (V)	Electrolyte concentration (% by wt)	Total time (min)	Shorts in switch (no)	Penetration rate (mm/min)
1	63.5	11.75	23.49	0	> feed rate
2	80.5	11.75	25.64	0	> feed rate
3	63.5	20.24	35.81	8	< feed rate
4	80.5	20.24	24.55	0	> feed rate
5	60	16	62.91	24	< feed rate
6	84	16	25.68	2	< feed rate
7	72	10	23.72	0	> feed rate
8	72	22	25.60	1	< feed rate
9	72	16	26.69	0	> feed rate
10	72	16	26.69	2	< feed rate
11	72	16	26.85	0	> feed rate
12	72	16	26.71	2	< feed rate
13	72	16	26.33	0	> feed rate

4.2 Overcut

Overcut of the machined groove has been calculated as shown in Fig 4.2 using the equation given below

Overcut = (Kerf width – Tool thickness)/2 (1)

Overcut of the machined groove was measured by a shadowgraph with 50 times magnification. Overcut obtained at different experimental conditions is listed in Table 4.2. Higher material removal rate in ECSMWRP because of the combined effect of sparking and chemical reaction, causes the more overcut in ECSMWRP.

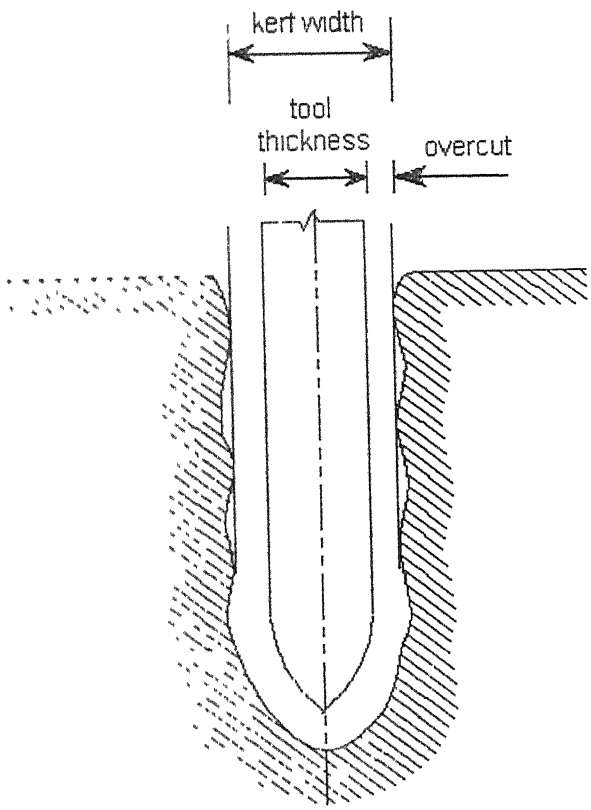

Fig 4.2 Schematic diagram of the groove

Table 4.2 Overcut values in ECSM process

Voltage (V)	Electrolyte concentration (% by wt.)	Kerf width (mm)		Overcut (mm)	
		ECSSMWDP	ECSMWRP	ECSMWDP	ECSMWRP
63.5	11.76	0.61	674	0.055	0.087
80.5	11.76	0.665	1.066	0.082	0.283
63.5	20.24	0.548	980	0.024	0.240
80.5	20.24	0.715	1.270	0.107	0.388
60	16	0.666	921	0.083	0.210
84	16	0.771	901	0.135	0.200
72	10	0.716	77	0.108	0.135
72	22	0.69	808	0.095	0.154
72	16	0.637	747	0.068	0.1235
72	16	0.65	824	0.075	0.162
72	16	0.68	686	0.090	0.093
72	16	0.662	700	0.081	0.1

4.3 Surface finish

Surface finish was measured by surf analyzer along cutting direction randomly at six different places (Appendix-2) Average values are Table 4.3 Surface produced in ECSM process is not uniform because of the random spark generation and unknown behavior of dissolution of quartz by chemical action in ECSMWRP

Table 4.3 Surface finish in ECSM process

Voltage(V)	Electrolyte concentration (% by wt)	Average Surface finish (R_a, µm)	
		ECSMWDP	ECSMWRP
63.5	11.75	5.983	8.383
80.5	11.75	9.816	12.066
63.5	20.24	9.116	7.083
80.5	20.24	7.7	11.983
60	16	12.316	9.016
84	16	9.4	9.116
72	10	8.55	14.85
72	22	13.683	5.183
72	16	6.266	5.6
72	16	10.983	8.233
72	16	7.6	6.8
72	16	8.566	5.016

Fig 4.3 Surface finish of the machined surface measured by surf analyzer (ECSMWDP)

(FILE NOT SAVED)

FEDERAL PRODUCTS CO

XXX-YYY

J EMPLOYEE

0.80 mm
0.80 mm
ANSI 2-RC
3.25 mm/sec
+/-500 Um
1:1
0.66 mm
Normal
0.05 mm/div
+/-5.0 Um

0.05 mm/div
+/-5.00 Um
(1.00 Um/div)

1 div = 1 cm

PARAMETER RESULTS

PROFILE		
PRa		Um
PRq		Um
Pt		Um
ROUGHNESS		
Ra	2.7	Um
Rq	3.3	Um
Rv	19.8	Um

WAVINESS

Fig 4.1 Surface finish of the machined surface measured by surf analyzer (ECSMWRP)

4.4 Tool Wear

Tool wear rate in ECSMWRP was negligible compared to ECSMWDP (Table 3 1) In ECSMWDP heat generated by sparking causes the melting and vaporization of tool material (cathode) But by the electrochemical action copper is deposited on cathode ($Cu^{++} + 2e^{-} \rightarrow Cu$) Hence negligible tool wear is obtained in ECSMWDP In ECSMWRP, tool is anode By electrochemical action copper is dissolved from anode Therefore sparking and anodic dissolution of copper causes high tool wear in ECSMWRP Higher rate of chemical reaction and high spark intensity at work-piece tool interface causes the formation of deep crater on the tool at machining zone (Figs 4 5, and 4 6)

(a)

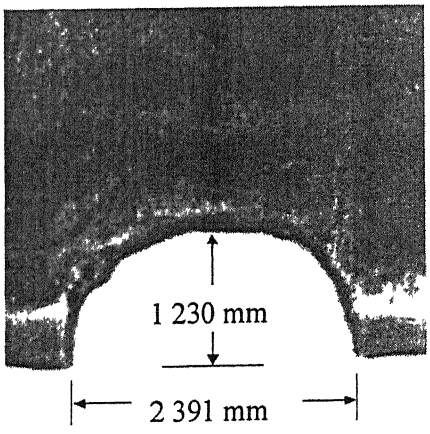

(b)

Fig 4 5 Tool shape after machining (voltage 72 V, electrolyte concentration 10% by wt , machining time 23 72 min), [(a) after cutting by ECSMWDP, (b) after cutting by ECSMWRP]

(a)

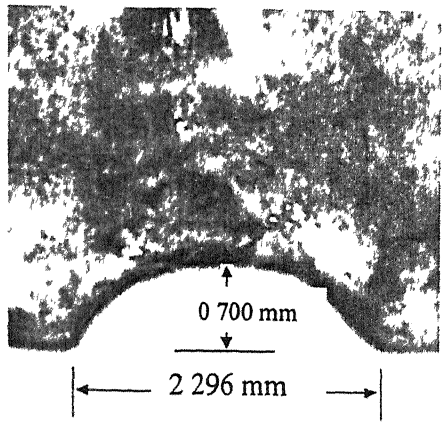

(b)

Fig 4 6 Tool Shape after machining (voltage 63 5, electrolyte concentration 11 76% by wt , machining time 23 49 min), [(a) after cutting by ECSMWDP, (b) after cutting by ECSMWRP]

4.5 Surface integrity of the machined surface

SEM photograph of the machined surface at high voltage was taken (84 V, 16 % electrolyte concentration) to study the surface integrity of the machined surface Cracks on the machined surface due to random thermal stress are clearly visible on the machined surface for

ECSMWDP (Fig 4 7) Magnified view of the machined profile clearly shows the difference in the surface integrity for the machined profile of ECSMWDP and ECSMWRP (Fig 4 8) Magnified view of the machined surface shows that in ECSMWDP surface is smooth and micro cracks on the surface are visible In ECSMWRP, the cracks on the machined surface are not visible and surface is rough This indicates chemical etching of the grains in ECSMWRP There fore SEM photographs it can be concluded that there is the difference in the mode of material removal in ECSMWDP and ECSMWRP

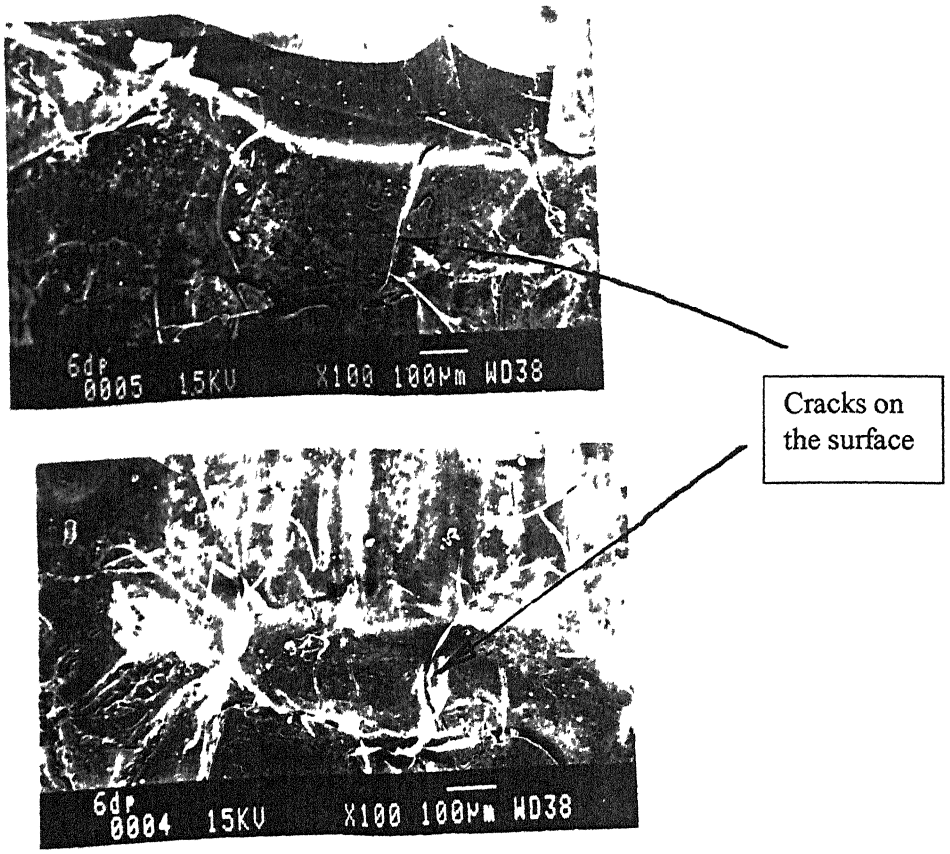

Fig 4 7 Cracks on the machined surface for ECSMWDP process
(Voltage 84 V, Electrolyte concentration 16 % by wt)

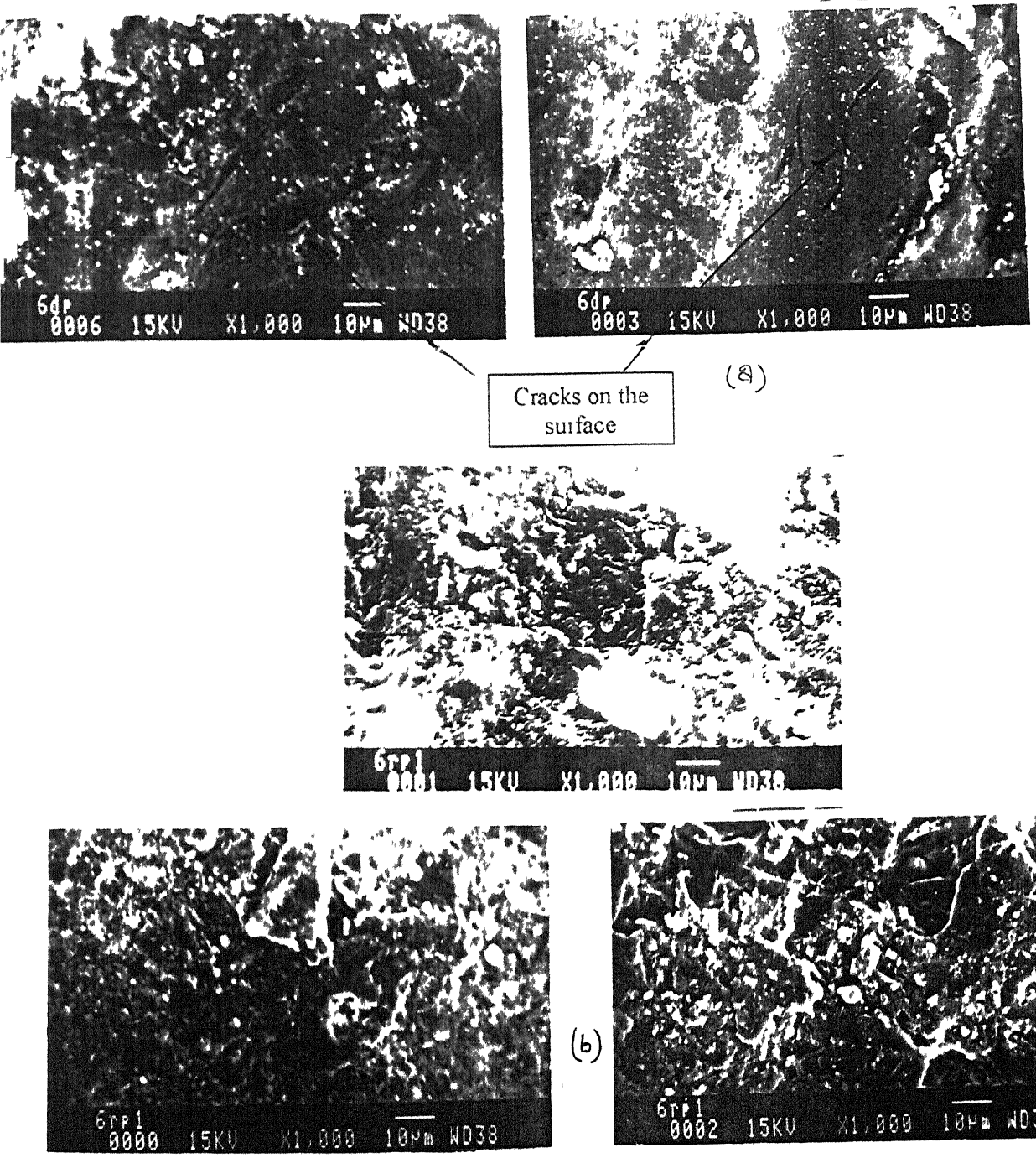

Fig 4 8 Magnified view of the machined surface at different locations (Voltage 80 V, electrolyte concentration 22 % by wt) [(a) ECSMWDP (smooth surface and cracks are visible), (b) ECSMWRP (rough surface and cracks are not visible)]

Chapter 5

MACHINING BY SMALL ELECTRODES

The concept of the ECSM is that size of the tool (cathode in case of ECSMWDP and anode in case of ECSMWRP) is much smaller than auxiliary electrode (anode in case of ECSMWDP and cathode in case of ECSMWRP) Very high current density at tool generates more no of gas bubbles Across the bubble, high potential gradient is developed But no quantitative data is available on, how big auxiliary electrode should be compared to the tool electrode In this chapter, experimental observations on the cutting of quartz plate by using small electrodes have been reported

5.1 ECSMWDP with small electrode

In ECSMWDP, cathode surface is shielded by hydrogen gas bubbles This causes high resistance to current flow A high electric field of the order of 10^7 V/m [9] is generated across the cathode tip and H_2 bubbles, resulting in arc discharge within the gas bubbles Basic electrochemical reaction of hydrogen gas evolution at cathode in electrolytic cell is

$$2H^+ + 2e^- \rightarrow H_2\uparrow$$

Amount of hydrogen generation depends on electron transfer rate at cathode electrolyte interface, properties of electrolyte and electrodes, applied voltage, etc Rate of transfer of electron from cathode to electrolyte and electrolyte to anode is equal If electron transfer rate at anode electrolyte interface is less compared to cathode electrolyte interface, then electron transfer rate at cathode electrolyte interface will also decrease Therefore, rate of hydrogen bubbles generation at cathode will also decrease because of less amount of electrons flow due to limited capacity of electrons transfer rate at anode electrolyte interface Experimental observation shows that for copper electrode and NaOH as electrolyte, spark intensity at small

cathode is not affected by small size of anode Therefore, if we replace large anode plate by an anode tip (Fig 5 1) cutting speed is not affected at cathode

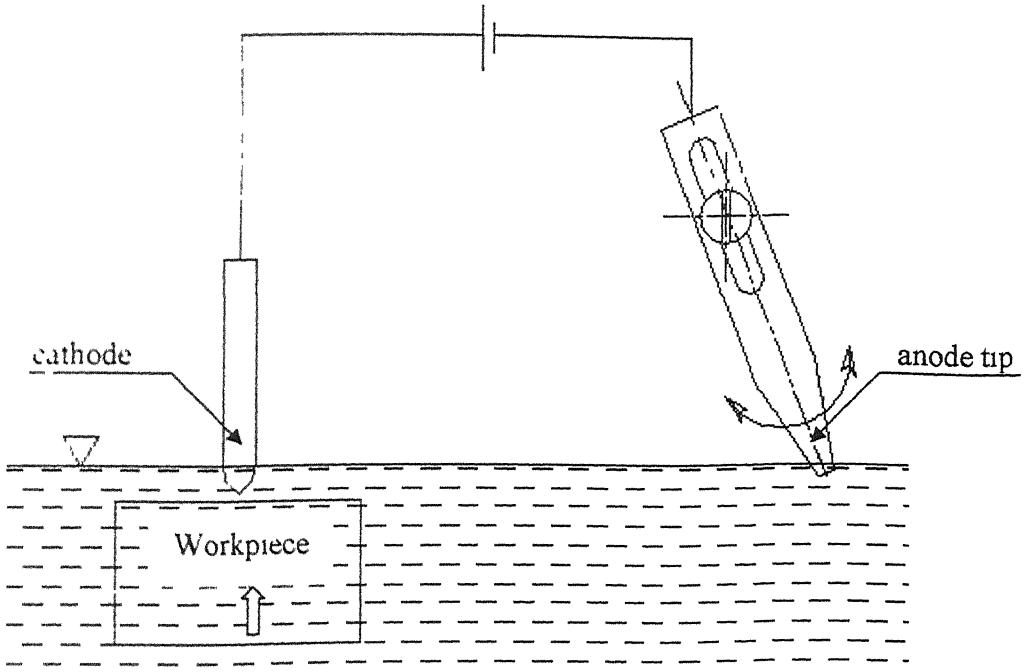

Fig 5 1 ECSMWDP with small electrodes

5.2 ECSMWRP with small electrode

Polarity of the setup shown in Fig 5 1 was changed and used for this purpose Initially a small portion of the cathode tip was dipped into electrolyte External potential was applied across the electrodes Sparking occurred at cathode tip due to high charge density at cathode tip In this case, at anode tip cutting of the quartz plate was not taking place Now cathode tip was gradually dipped into electrolyte Sparking at cathode tip would suddenly stop In this case quartz under anode tip start getting machined

Total potential drop between electrodes = Potential drop at cathode tip + Potential drop due to resistance of the electrolyte between electrodes + Potential drop at anode tip

Sparking occurs due to resistance to current flow at cathode tip and anode tip It causes high voltage drop across that zone Therefore if sparking occurs at cathode tip, high voltage drop occurs at cathode tip and sufficient voltage is not available near the anode tip for machining That's why cutting was not taking place at anode when there is sparking at cathode If there is no sparking at cathode tip, less potential drops near cathode Therefore high potential is available near anode tip that causes high rate of dissolution of quartz near anode tip

5.3 Machining at both the electrodes

In earlier work, ECSMWDP and ECSMWRP have been separately applied for cutting of quartz plate It also has been observed that machining is possible even though auxiliary electrode is small (5 1, 5 2) Therefore in ECSM process, tool electrode (cathode in ECSMWDP and anode in ECSMWRP) should be small and auxiliary electrode also may be small or large An attempt has been made to machine simultaneously at both the electrodes by using both the electrodes of small size Schematic diagram of the setup is shown in Fig 5 2 In this case both the electrodes work as tool and machining occur at both the electrodes

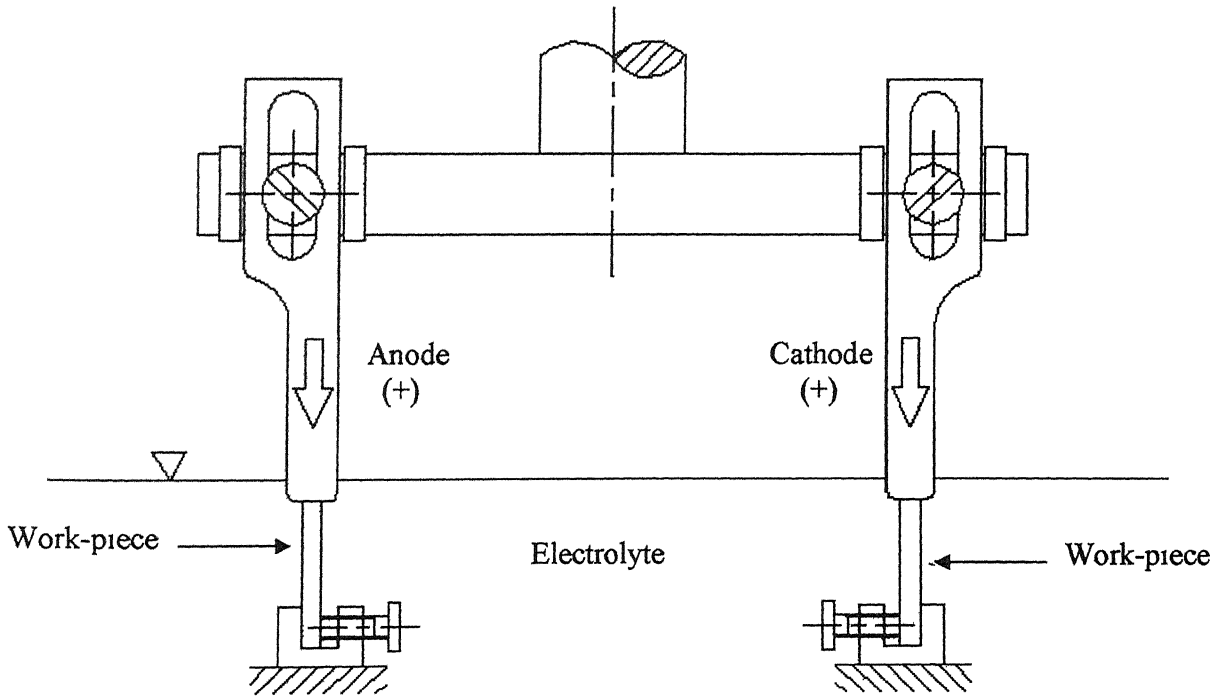

Fig 5 2 Machining at both the electrodes

5.3.1 Working principle for machining at both electrodes

While machining at both the electrode, it has been observed that sparking occurs only at one electrode at a time and spark zone keeps shifting from cathode tip to anode tip and vice versa (Fig 5.3) Resistance to current flow due to evolution of gas bubbles and vapour bubbles at both the electrodes leads to sparking at electrode tips When sparking occurs at one electrode, at that time shielding of other electrode by gas and vapour bubbles takes place Thus increases the resistance near that electrode When resistance becomes sufficiently high, sparking zone shifts to that electrode Thus shifting of sparking zone occurs between electrodes When sparking zone is at cathode tip, the process is ECSMWDP When sparking occurs at anode tip, the process is ECSMWRP Thus machining occurs at both the electrodes

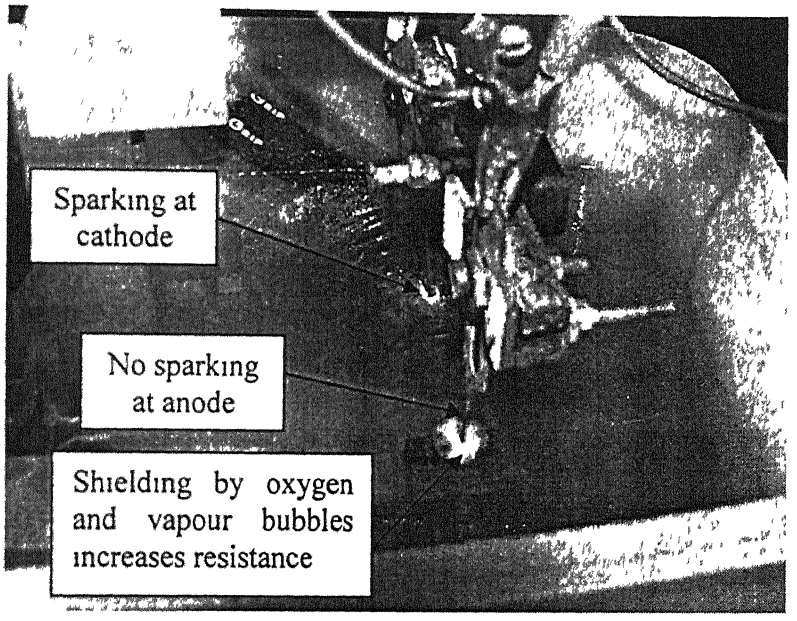

(a)

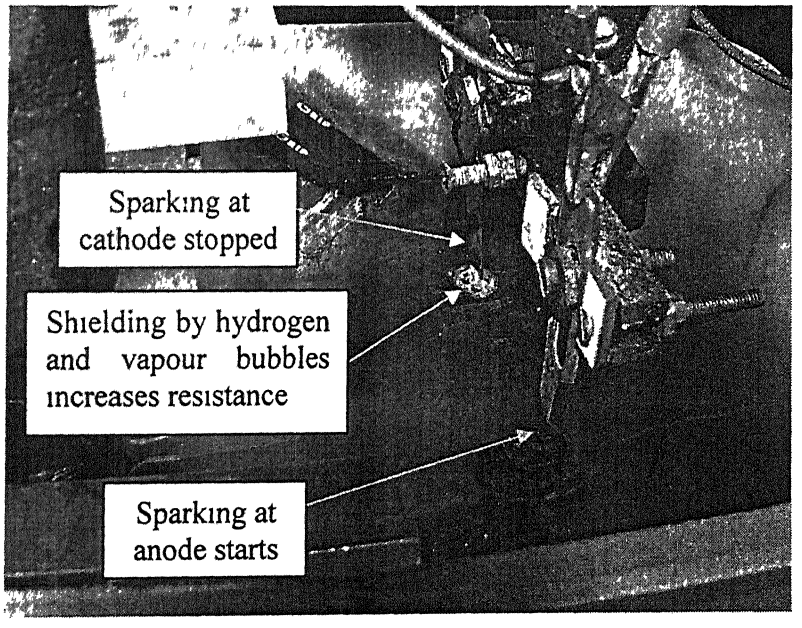

(b)

Fig 5 3 Shifting of sparking zone between electrodes
[(a) sparking at cathode, (b) sparking at anode]

5.3 2 Experimental results

It has been observed that at a time, sparking occurs only at one electrode for the range of (60-80 V) If voltage is increased beyond 80 V then, so that spark always occurs at both the electrodes rather than shifting between electrodes, work-piece cracks due to high thermal stresses and also melting of the tool may occur due to high heat generation (Fig 5.4)

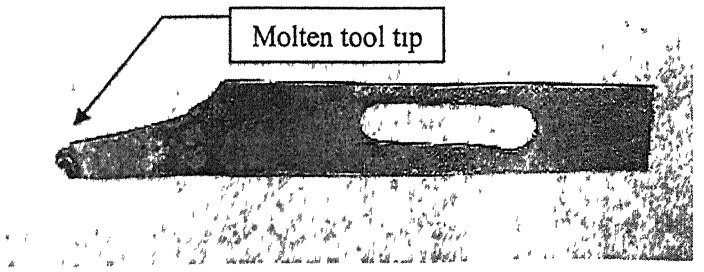

Fig 5.4 Melting of tool tip at high voltage (110 V, electrolyte concentration 22% by wt)

Three experiments were conducted at voltage range of (60-80 V) to study the process performance. Details of the cutting conditions are listed in Table 5.1 After cutting the groove, magnified view of the profile was taken by shadowgraph (Figs 5 6, and 5 7) For the measurement of kerf width and surface roughness along the machined depth, whole length of the groove was divided into five equal divisions. Width of the groove was measured at the locations 1, 2, 3 and 4 (Fig 5 6). Two extreme points (location 0 and location 5) were not counted because in some cases, kerf width at top is much higher and kerf width at bottom is much lower compared to average kerf width Surface roughness was measured near those points, on surface of the kerf. The kerf width and surface roughness values are listed in Table 5 2. Experimental results show that penetration rate is almost same at both the electrodes for all the experiments. Negative tool in general produces better quality Kerf (less overcut and low surface roughness) compared to positive tool, but material removal rate is higher for positive than negative tool (almost same penetration rate but higher overcut

compared to negative tool) Fig 5 8 and Fig 5 9 shows penetration and kerf width increases with increased voltage for both tools, because of high discharge energy for sparking and high rate of chemical reactions at high voltage causes higher material removal Average Surface roughness also increases with voltage (Fig 5 10). Because at higher voltage high energy is discharged by sparking, this causes deep crater on machined surface Hence surface roughness increases with voltage for the machined cavity at cathode For anode at high voltage, higher rate of chemical dissolution of quartz occurs and energy discharged by sparking is also more Therefore increased material removal rate at higher voltage causes high surface roughness

Table 5 1 Cutting conditions for machining at both electrodes
Electrolyte concentration= 22 % by wt.
Electrolyte temperature = 30 ^{0} C
Inter-electrode gap= 60 mm
Width of electrodes= 5 mm
Thickness of electrodes = 0.5 mm
Workpiece thickness = 2 mm

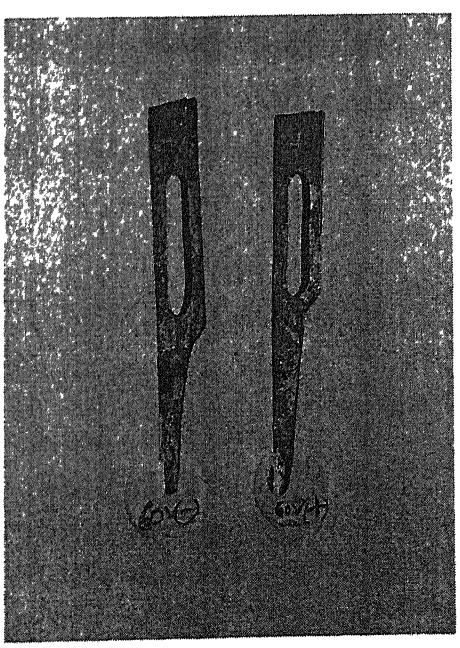

Fig.5.5 Tool and workpiece after machining at both electrodes

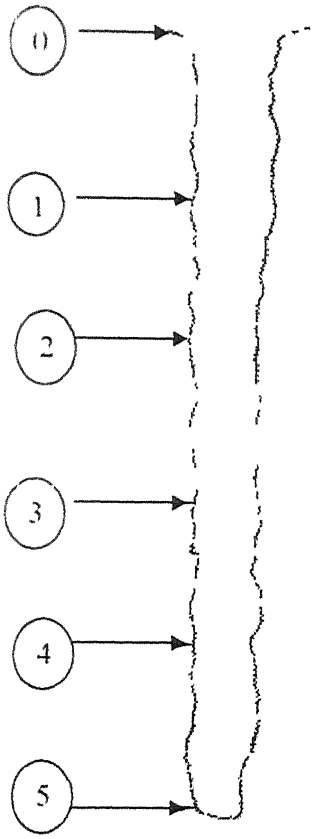

Fig 5 6 Magnified view of the kerf and locations for the measurements of kerf width

Table 5 2 Kerf width and surface roughness at different locations

Location on groove	Kerf width (mm)						Surface roughness (R_a, μm)					
	60 V		70 V		80 V		60 V		70 V		80 V	
	Tool (-)	Tool (+)	Tool (-)	Tool (+)	Tool (-)	Tool (+)	Tool (-)	Tool (+)	Tool (-)	Tool (+)	Tool (-)	Tool (+)
1	0 663	0 963	0 917	1 175	0 93	0 944	7 7	10 1	9	6 4	14 1	11 1
2	0 565	0 715	0 725	0 875	0 797	0 89	9 2	8 4	9 9	13	9 7	9 8
3	0 575	0 54	0 675	0 72	0.759	0 925	5 7	7 7	3 2	7 2	11 9	9 4
4	0 585	0 51	0 76	0 515	0 718	0 971	3 4	6 4	8 3	14 4	4	13 9
Average	0 597	0 682	0 769	0 821	0 801	0 932	6 5	8 15	7 6	10 25	9 925	11 05

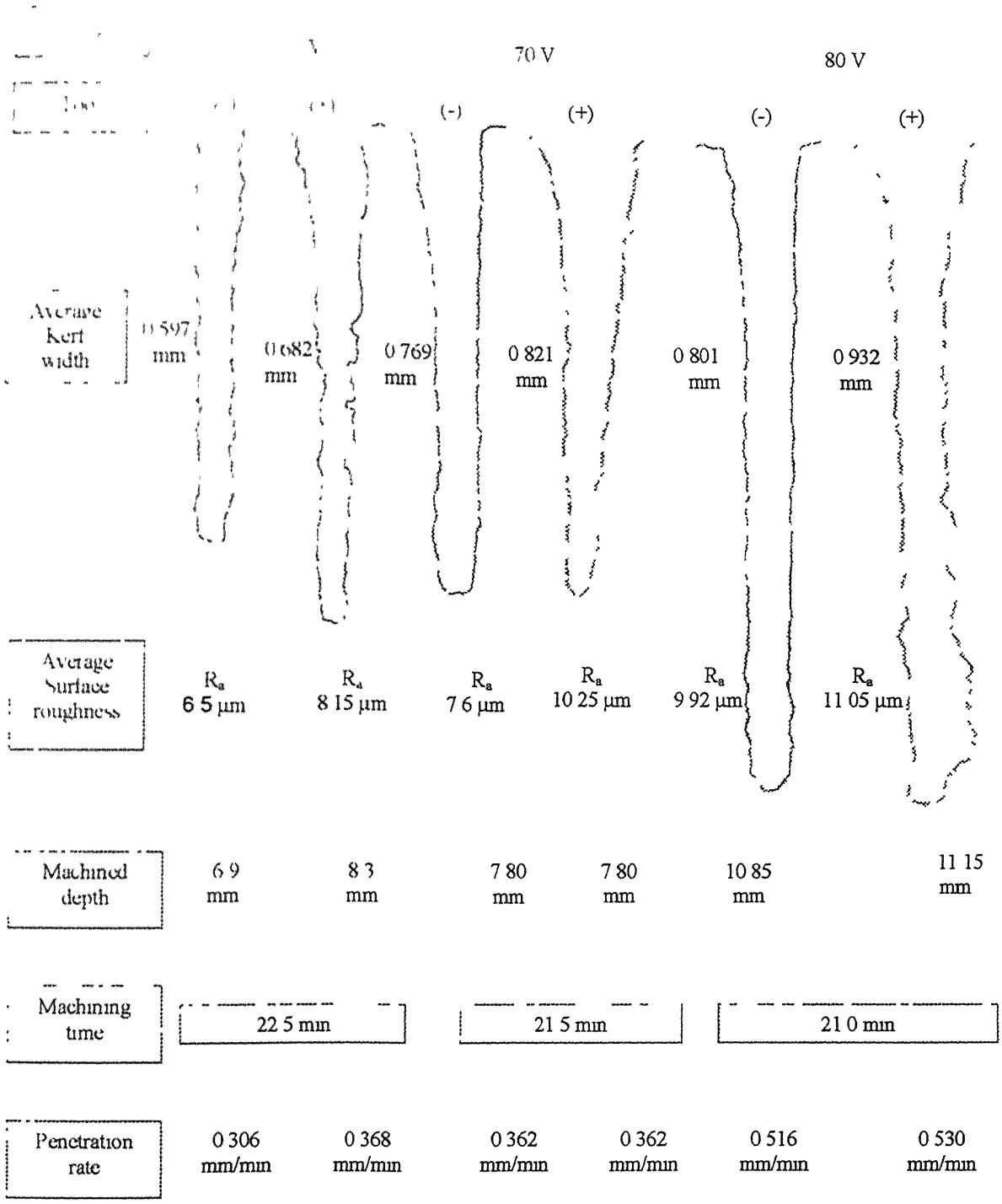

Fig 5 7 Enlarged view of the machined grooves from shadowgraph (Magnification 20 times)

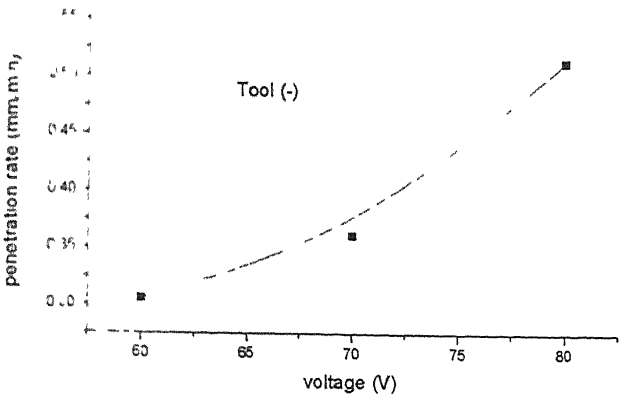

(a)

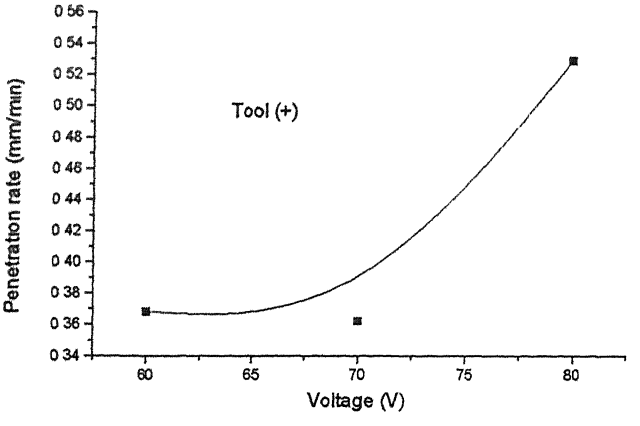

(b)

Fig 5 8 Variation of penetration rate with voltage
[(a) penetration rate at cathode, (b) penetration rate at anode]

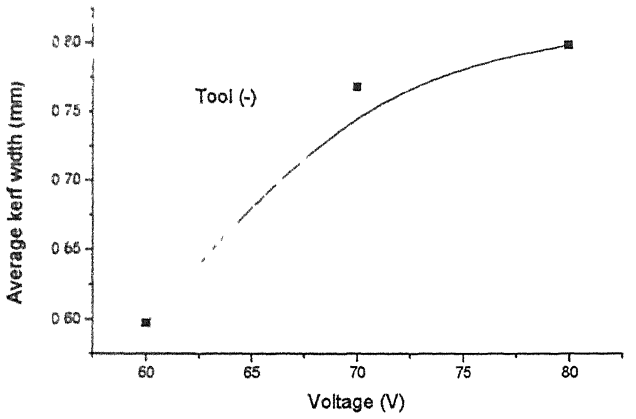

(a)

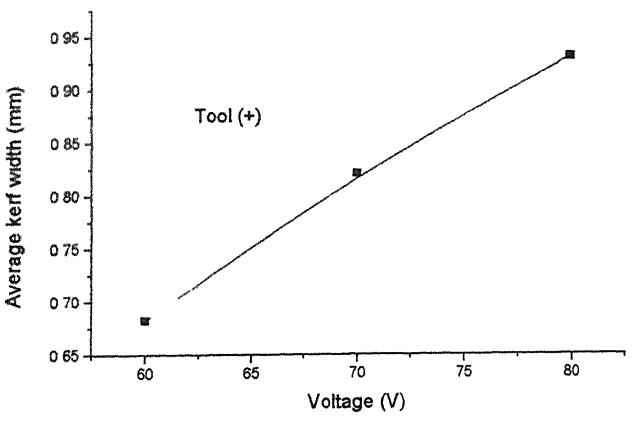

(b)

Fig 5.9 Variation of average kerf width with voltage [(a) average kerf width for the cavity at cathode, (b) average kerf width for the cavity at anode]

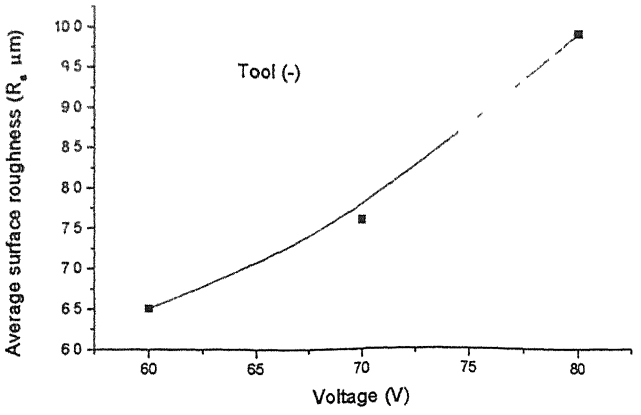

(a)

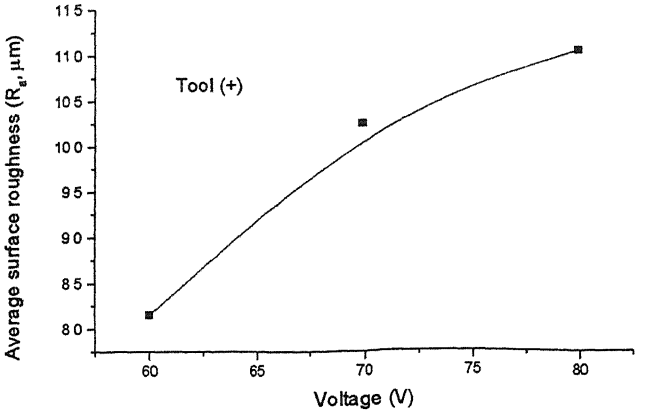

(b)

Fig 5.10 Variation of average surface roughness with voltage [(a) average surface roughness for the cavity at cathode, (b) average surface roughness for the cavity at anode]

Chapter 6

CONCLUSIONS

In the present work experimental investigations on the performance of ECSM process for cutting quartz plate and chemical analysis of the reaction products have been carried out Cutting using small electrode also has been successfully applied From this study following conclusions can be made

1 Electrochemical spark machining can be successfully used for cutting ceramic plate

2 Controlled feed to work-piece, and sharp tool produce better quality of machined profile

3 ECSMWRP cuts quartz plate at faster rate compared to ECSMWDP, but produces higher overcut and higher tool wear

4 Material removal in ECSMWRP is due to chemical action also Chemical analysis of reaction products also confirms the dissolution of quartz into NaOH solution

5 Cutting performance in ECSMWDP and ECSMWRP is not affected by small size anode However if there is sparking at cathode in ECSMWRP current flowing through the circuit does not participate in machining

6 Both the electrodes simultaneous can be used as tool (ECSMWDP + ECSMWRP) If we use only one electrode as tool at a time, size of the other electrode should be such that sparking zone always confined near the small electrode for machining

Chapter 7

SCOPE FOR FUTURE WORK

Most of the fundamental aspects of ECSM process including material removal mechanism, generation of controlled sparking, controlling of the process performance etc , are yet to be understood Further research is needed in the following areas for making the cutting process commercially viable

1 In this work ECSM process has been applied for cutting thin plate (~2 mm) ECSM process can be applied for cutting thick sheets by using small size tool and giving additional movement to tool or work-piece along horizontal plane

2 From Experimental observation and from chemical analysis it can be concluded that quartz dissolves into NaOH solution by chemical action However, rate of dissolution, influence of other factors like inter electrode gap, electrolyte flow, electrolyte level above the tool tip, etc , have not been studied

3 Optimization of process parameters are needed for better control of the process

4 Further work is needed to study the feasibility study of simultaneous application of ECSMWDP and ECSMWRP

5 To reduce tool wear in ECSMWRP, higher electropositive electrode material can be used

6 Machining performance using pulsed power supply and coated tool needs to be investigated

REFERENCES

1 Cook N H, Foote G B, Jordan P, Kalyani B N, Experimental studies in electro-machining, Transaction of the ASME Journal of Engineering for Industry, Nov 1973, PP 945-950

2 Allesu K, Electrochemical discharge phenomena in manufacturing process, Ph D thesis, IIT Kanpur, 1988

3 Jain V K, Rao P S, Choudhary S K, Rajukar K P, Experimental investigations into traveling wire electrochemical spark machining (TWECSM) of composites, Transaction of the ASME Journal of Engineering for Industry, Vol 113, Feb 1991, PP 75-84

4 Raghuram V, Pramila T, Srinivasa Y G, Narayanswamy, Effect of circuit parameters on the electrolytes in electrochemical discharge phenomenon, Journal of Materials Processing Technology, Vol 52, (1995), PP 289-300

5 Singh Y P, Jain V K, Kumar P, Agarwal D C, Machining piezoelectric (PZT) ceramics using an electrochemical spark machining (ECSM) process, Journal of Materials Processing Technology, Vol 58, (1996), PP 24-31

6 Gautam N and Jain V K, Experimental investigations into ECSD process using various tool kinematics, International Journal of Machine Tools and Manufacture, Vol 38, No 1-2, (1998), PP 15-27

7 Basak I, Ghosh A, Mechanism of material removal in electrochemical discharge machining a theoretical model and experimental verification, Journal of Materials Processing technology, Vol 71, (1997), PP 350-359

8 Singh M, Effect of porosity and glass content on machining of alumina ceramics by electrochemical spark machining (ECSM), M Tech thesis, IIT kanpur, 1997

9 Jain V K, Dixit P M, Pandey P M, On the analysis of the electrochemical spark machining process, International Journal of Machine Tools and Manufacture, Vol 39, (1999), PP 165-186

10 Bhattacharya B, Doloi B N, Sorkel S K, Experimental investigations into electrochemical discharge machining (ECDM) of non-conductive ceramic materials, Journal of Materials Processing Technology, Vol 95, (1999), PP 145-154

11 Doloi B , Bhattacharyya, Sorkel S K , Optimization of electrochemical discharge machining process for machining silicon nitride ceramics, Proceeding of National Symposium on Manufacturing Engineering in Twenty First Century, IIT kanpur, Mar 2001, PP 117-120

12 Jain V K , Chack S , Electrochemical spark trepanning of alumina and quartz, Machining Science and Technology, Vol 4, No 2, (2000) PP 277-290

13 Jain V K , Choudhury S K , Ramesh K M., On the machining of alumina and glass, International Journal of Machine Tools and Manufacture, Vol 42, (2002), PP 1269-1276

14 Kulkarni A , Sharan R , Lal G K , An Experimental study of discharge mechanism in electrochemical discharge machining, International Journal of Machine Tools and Manufacture, Vol 42, No 10, (2002), PP 121-1128

15 Gautam N , Experimental investigations for enhancement of ECDM process capabilities using various tool kinematics, M Tech Thesis, 1995

16 Anderson P H , Use of a PC printerport for control and data acquisition, http //et nmsu edu/~etti/fall96/computer/printer/printer html

17 Montegomery D C , Design and analysis of experiments, John Wiley & Sons (Asia) Pte Ltd , 5th edition

18 Coochran W C , Cox G M , Experimental designs, Asia Publishing House, 2nd edition

19 Mcgeough J A , Principles of electrochemical machining, Chapman and Hall, London, 1984

20 Debarr A E , Oliver D A , Electrochemical machining, Macdonald, London, 1967

21 Glasstone S , An introduction to electrochemistry, D Vannostrand, 1960

22 Windholtz M , Budavari S , Lorrine Y S , Margaret N F , The merck index, Merck & Co INC , 1976

23 Vivek V N , Jain V K , Travelling wire electro-chemical spark machining (TW-ECSM) of thick sheets of kevler-epoxy composites, 16th All India Manufacturing Technology Design and Research Conference, Dec 8-10, (1994), PP 672-677

24 Tandon S , Jain V K , Kumar P , Rajukar K P , Investigations into machining of composites, Precision Engineering, Vol 12, No 4, Oct 1990, PP 227- 238

25 Jain V K , Tandon S , Kumar P , Experimental investigations into electrochemical spark machining of composites, Transaction of the ASME Journal of Engineering for Industry, Vol 112, May 1990, PP 194-196

26 Basak I , Ghosh A , Mechanism of spark generation during electrochemical discharge machining a theoretical model and experimental verification, Journal of Material Processing technology, Vol 62, (1997), PP 46-53

APPENDIX-1

Program used for Experiment

```
/* Final program for experiment */
#include <stdio.h>
#include <dos.h>
#include <conio.h>
#include <math.h>

#define DATA 0x0378
#define STATUS DATA+1
#define CONTROL DATA+2
#define REV_ROT 15.0

void main ()
{
     int sw;
     float fdelay,rdelay,j, distance,m,y,z,forward;
     printf("Enter delay for feed   \n"),
     scanf("%f",&fdelay);
     printf("Enter delay for reverse direction. ...\n");
     scanf("%f",&rdelay);
     forward=0.0;
     z=0.0,
     y=0.0;
     m=0.0;
while(1)
{
   sw=inportb(STATUS);
   printf(" T_R_ROT %f\tT-F_Rot %f",y,forward);
```

```
switch (sw

case 127:
  z=0.0;
  outportb (DATA, 0x00),
  delay (fdelay);
  outportb (DATA, 0x05);
  delay (fdelay);
  m=m+0.005;
  printf(" SW_is %d\ FWD_ROT %f\n",sw,m);
  forward=forward+0.005;


  break;

case 255:
  m=0.0;
  distance=200*(REV_ROT),
  for(j=0;j<distance;j++)
  {
       outportb (DATA, 0x02);
       delay (rdelay);
       outportb (DATA, 0x07),
       delay (rdelay);
       y=y+0.005;
       z=z+0.005,
  printf("Rev_Rot %f\tT_R_ROT
%f\tT_F_Rot\t%f\n",z,y,forward);

  }
  break;
```

```
    [illegible]
      ox 1 ,
      break;
```

APPENDIX-2

Surface finish in ECSM process

Table A2 1 Surface finish in ECSMWDP

Voltage (V)	Electrolyte concentration (% by wt)	Surface finish (R_a, μm)						Average (R_a, μm)
63 5	11 76	2 1	3 2	3 3	4 8	11 2	11 3	5 98
80 5	11 76	6 6	7 9	8 4	7 9	11 2	16 9	9 81
63 5	20 24	4 1	4 5	9 3	10 2	11 6	15	9 11
80 5	20 24	5 6	6	6 3	6 8	9 9	11 6	7 7
60	16	7 9	11 3	12 5	13 4	13 6	15 2	12 31
84	16	6 2	7 5	9 2	9 3	9 9	14 3	9 4
72	10	5	5 5	7 1	8 2	12 3	13 2	8 55
72	16	8 2	9 7	12 8	15 7	17 7	18	13 68
72	16	3 7	4 5	5 3	7 6	7 9	8 6	6 26
0	16	7 6	8 3	9 6	10 5	13 2	16 7	10 98
0	16	3 5	3 6	4 7	7 9	12 5	13 4	7 6
0	16	4 5	5 1	6 3	10 4	11 9	13 2	8 56

Table A2 2 Surface finish in ECSMWRP

Voltage(V)	Electrolyte concentration (% by wt)	Surface finish (R_a, μm)						Average (R_a, μm)
63 5	11 75	3 4	6 5	7 2	9 4	9 6	14 2	8 383
80 5	11 75	5 8	8 4	12	12 3	16 3	17 6	12 066
63 5	20 24	4 2	5 2	5 8	6 8	8 3	12 2	7 0833
80 5	20 24	6 8	9 6	11	11 7	15 1	17 7	11 983
60	16	3 8	6 3	8 9	9 6	12 7	12 8	9 016
84	16	3 3	4 4	5 3	8 9	11 4	21 4	9 116
72	10	9 7	11 6	12 7	14	19 4	21 7	14 85
72	22	2 7	3 6	3 6	6 9	7	7 3	5 183
72	16	4 2	4 5	5 8	5 9	6	7 2	5 6
72	16	4 6	4 8	7 5	8 5	10 3	13 7	8 233
72	16	4	4 3	4 5	6 3	9 7	12	6 8
72	16	10 9	11 4	13	13 1	13 3	14 2	5 016